การโดป CeO_2 บนตัวเร่งปฏิกิริยา V_2O_5-TiO_2 ในปฏิกิริยารีดักชันแบบเลือกเกิดที่ใช้ตัวเร่งปฏิกิริยาของก๊าซไนโตรเจนออกไซด์โดยแอมโมเนียที่อุณหภูมิต่ำ

นายวราวุฒิ ไวยวาสา

วิทยานิพนธ์นี้เป็นส่วนหนึ่งของการศึกษาตามหลักสูตรปริญญาวิศวกรรมศาสตรมหาบัณฑิต
สาขาวิชาวิศวกรรมเคมี ภาควิชาวิศวกรรมเคมี
คณะวิศวกรรมศาสตร์ จุฬาลงกรณ์มหาวิทยาลัย
ปีการศึกษา 2557

DOPING OF CeO_2 IN V_2O_5-TiO_2 CATALYST FOR LOW-TEMPERATURE SELECTIVE CATALYTIC REDUCTION OF NITROGEN OXIDE BY AMMONIA

Mr. Warawut Waiwasa

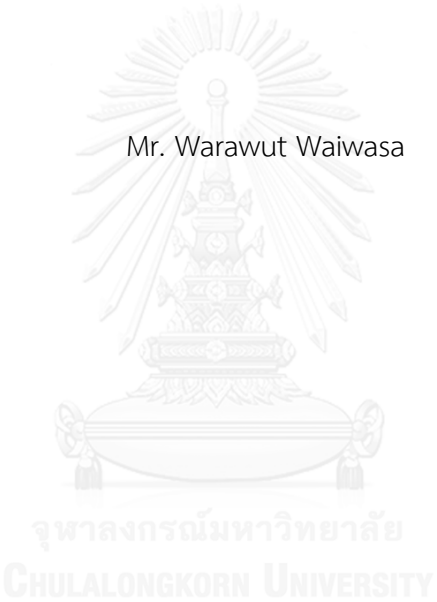

A Thesis Submitted in Partial Fulfillment of the Requirements
for the Degree of Master of Engineering Program in Chemical Engineering
Department of Chemical Engineering
Faculty of Engineering
Chulalongkorn University
Academic Year 2014

Thesis Title	DOPING OF CeO_2 IN V_2O_5-TiO_2 CATALYST FOR LOW-TEMPERATURE SELECTIVE CATALYTIC REDUCTION OF NITROGEN OXIDE BY AMMONIA
By	Mr. Warawut Waiwasa
Field of Study	Chemical Engineering
Thesis Advisor	Akawat Sirisuk, Ph.D.

Accepted by the Faculty of Engineering, Chulalongkorn University in Partial Fulfillment of the Requirements for the Master's Degree

.....Dean of the Faculty of Engineering

(Professor Bundhit Eua-arporn, Dr.Ing.)

THESIS COMMITTEE

.....Chairman

(Associate ProfessorTawatchai Charinpanitkul, Ph.D.)

.....Thesis Advisor

(Akawat Sirisuk, Ph.D.)

.....Examiner

(Palang Bumroongsakulsawat, Ph.D.)

.....External Examiner

(Kanokwan Ngaosuwan, D.Eng.)

วราวุฒิ ไวยวาสา : การโดป CeO_2 บนตัวเร่งปฏิกิริยา V_2O_5-TiO_2 ในปฏิกิริยารีดักชันแบบเลือกเกิดที่ใช้ตัวเร่งปฏิกิริยาของก๊าซไนโตรเจนออกไซด์โดยแอมโมเนียที่อุณหภูมิต่ำ (DOPING OF CeO_2 IN V_2O_5-TiO_2 CATALYST FOR LOW-TEMPERATURE SELECTIVE CATALYTIC REDUCTION OF NITROGEN OXIDE BY AMMONIA) อ.ที่ปรึกษาวิทยานิพนธ์หลัก: ดร.อัครวัต ศิริสุข, 84 หน้า.

งานวิจัยนี้ทำการศึกษาปฏิกิริยารีดักชันแบบเลือกเกิดที่ใช้ตัวเร่งปฏิกิริยาของก๊าซไนโตรเจนออกไซด์โดยแอมโมเนีย และยังมีการศึกษาปฏิกิริยาออกซิเดชันของแอมโมเนียซึ่งเป็นปฏิกิริยาข้างเคียง การเตรียมตัวรองรับไททาเนียจะเตรียมโดยใช้วิธีโซลเจล และทำการการโดปโลหะวานาเดียมและซีเรียมโดยใช้วิธีเคลือบฝังแบบเปียกพอดีรูพรุน ปริมาณของซีเรียมและวานาเดียมจะอยู่ในช่วงร้อยละ 1 ถึง 7 โดยน้ำหนัก และ ร้อยละ5 ถึง 30 โดยน้ำหนัก ตามลำดับ ทำการวิเคราะห์ตัวเร่งปฏิกิริยาโดยใช้เทคนิค N_2 physisorption, ICP-OES, XRD และ NH_3-TPD การทดสอบตัวเร่งปฏิกิริยากระทำในช่วงอุณหภูมิ 120-450 องศาเซลเซียส จากการศึกษาพบว่าตัวเร่งปฏิกิริยาที่มีวานาเดียมร้อยละ 5 โดยน้ำหนัก และ ซีเรียมร้อยละ 30 โดยน้ำหนัก มีความเหมาะสมในการใช้งานที่อุณหภูมิต่ำ ซึ่งมีความว่องไวสูงสุดอยู่ที่อุณหภูมิ 250 องศาเซลเซียส ซึ่งพบว่าการเติมซีเรียมในตัวเร่งปฏิกิริยาจะไปเพิ่มในส่วนของพื้นที่ผิวของตัวเร่งปฏิกิริยา และ มีการดูดซับแอมโมเนียที่ดีเนื่องจากไปเพิ่มความเป็นกรดบนตัวเร่งปฏิกิริยา เหตผลดังกล่าวจึงทำให้ตัวเร่งปฏิกิริยามีประสิทธิภาพที่ดี ในส่วนของการศึกษาปฏิกิริยาออกซิเดชันของแอมโมเนีย พบว่าปฏิกิริยาออกซิเดชันของแอมโมเนียจะเกิดเพิ่มมากขึ้นเนื่องจากสองปัจจัยคือ ปัจจัยแรกคืออุณหภูมิ ปัจจัยต่อมาคือปริมาณวานาเดียมบนตัวเร่งปฏิกิริยา ซึ่งการการทดลองพบว่าการเติมซีเรียมในตัวเร่งปฏิกิริยานั้นจะสามารถไปยับยั้งการเกิดปฏิกิริยาออกซิเดชันของแอมโมเนียซึ่งมีผลทำให้ประสิทธิภาพของตัวเร่งปฏิกิริยาที่อุณหภูมิสูงนั้นยังคงมีประสิทธิภาพที่ดี ส่วนการศึกษาตัวเร่งปฏิกิริยาภายใต้สภาวะที่มีไอน้ำและซัลเฟอร์ไดออกไซด์ในระบบพบว่า การเติมซีเรียมลงในตัวเร่งปฏิกิริยาวานาเดียมนั้น คุณภาพของตัวเร่งปฏิกิริยายังสามารถมีความว่องไวที่ดีภายใต้สถาวะดังกล่าว

ภาควิชา วิศวกรรมเคมี ลายมือชื่อนิสิต .....

สาขาวิชา วิศวกรรมเคมี ลายมือชื่อ อ.ที่ปรึกษาหลัก .....

ปีการศึกษา 2557

5670367821 : MAJOR CHEMICAL ENGINEERING

KEYWORDS: SELECTIVE CATALYTIC REDUCTION / SOL-GEL METHOD / VANADIUM AND CERIUM CATALYST / AMMONIA OXIDATION REACTION

WARAWUT WAIWASA: DOPING OF CeO_2 IN V_2O_5-TiO_2 CATALYST FOR LOW-TEMPERATURE SELECTIVE CATALYTIC REDUCTION OF NITROGEN OXIDE BY AMMONIA. ADVISOR: AKAWAT SIRISUK, Ph.D., 84 pp.

This research investigated the selective catalytic reduction of NO by NH_3 over V_2O_5-CeO_2/TiO_2 catalyst at low temperature. Formation of nitrogen oxide from the ammonia oxidation reaction and SCR reaction was also investigated. Titanium dioxide support was prepared by a sol-gel method. Then vanadium and cerium were deposited via an incipient wetness impregnation method. The amounts of vanadium and cerium in the catalyst ranged from 1 to 7%wt and 5 to 30%wt, respectively. The catalysts were characterized by N_2 physisorption, ICP-OES, XRD and NH_3-TPD techniques. The testing of SCR activity of the catalyst was carried out in a tubular reactor at a temperature in the range of 120-450°C. From the result, the catalyst containing 5 %wt. V_2O_5, 30 %wt. CeO_2 showed superior SCR activity at low temperature and reached the highest activity at 250°C. The addition of CeO_2 increased the specific surface area and the total acid site of catalyst, resulting in high catalytic activity. The extent of ammonia oxidation increased as the reaction temperature and the vanadium content in catalysts increased. Addition of cerium to catalyst inhibited ammonia oxidation reaction and retained the SCR activity at high temperature. Furthermore, the addition of cerium oxide to the V_2O_5-TiO_2 catalyst yielded SCR catalysts an excellent resist to water vapor and sulfur dioxide under our test conditions.

Department:	Chemical Engineering	Student's Signature	.....
Field of Study:	Chemical Engineering	Advisor's Signature	.....
Academic Year:	2014		

ACKNOWLEDGEMENTS

The author would like to express his greatest gratitude and appreciation to his adviser, Dr. Akawat Sirisuk for his invaluable guidance, providing value suggestions and his kind supervision throughout this study. And thanks to Center of Excellence on Catalysis and Catalytic Reaction Engineering for supporting this research.

Finally. he would like to dedicate the achievement of this work to his parents who have always been the source of his suggestion, support and encouragement.

CONTENTS

Page

THAI ABSTRACT iv

ENGLISH ABSTRACT v

ACKNOWLEDGEMENTS vi

CONTENTS vii

LIST OF TABLE XI

LIST OF FIGURE XIII

CHAPTER l INTRODUCTION 1

CHAPTER II BACKGROUND INFORMATION 5

2.1 Nitrogen oxide (Roy et al., 2009, Gomez-Garcia et al., 2005) 5

2.2 NO_x Formation [Roy et al., 2009] 5

2.3 Selective catalytic reduction (SCR) of NO by ammonia 6

2.4 Mechanism of selective catalytic reduction for V_2O_5-base catalysts (Busca et al., 1998) 8

2.5 The active phases and the roles of the support and promoters in the commercial catalysts. (Busca et al., 1998) 9

2.6 The effect of the presence of H_2O and SO_2 on NO reduction 11

2.7 Effect of metal oxide for SCR 12

CHAPTER III EXPERIMENTAL 15

3.1. Catalyst preparation 15

3.1.1 Chemicals 15

3.1.2 Preparation of V_2O_5/TiO_2 and V_2O_5-CeO_2/TiO_2 catalyst powder 15

3.2 Characterization of catalyst 17

3.2.1 Surface area measurement 17

Page

3.2.2 X-ray diffraction (XRD) 17
3.2.3 Inductively Coupled Plasma-Optical Emission Spectroscopy (ICP-OES) 17
3.2.4 NH_3 temperature program desorption (NH_3-TPD) 17
3.3 Catalytic activity measurement 18
CHAPTER IV RESULTS AND DISCUSSION 21
4.1 Characterization of V_2O_5-TiO_2 and CeO_2-V_2O_5-TiO_2 catalysts 21
4.1.1 Composition of metal oxide contained in the catalyst 21
4.1.2 X-ray diffraction (XRD) 22
4.1.3 Specific surface area and crystallite size of the catalysts 24
4.1.4 Concentration of acid site of catalyst 25
4.2 Selective catalytic reduction of NO by NH_3 over V_2O_5-TiO_2 and CeO_2-V_2O_5/TiO_2 catalysts 27
4.2.1 Activity of V_2O_5/TiO_2 catalysts 28
4.2.2 Effect of CeO_2 on the activity of V_2O_5/TiO_2 catalyst 29
4.3 The formation of nitrogen oxide from ammonia oxidation reaction. 32
4.4 Effect of water vapor and sulfur dioxide on the catalysts. 37
4.4.1 Effect of sulfur dioxide on the activity of V_2O_5/TiO_2 and CeO_2-V_2O_5/TiO_2 catalysts. 37
4.4.2 Effect of water vapor on the activity of V_2O_5/TiO_2 and CeO_2-V_2O_5/TiO_2 catalysts. 40
4.4.3 Effect of water vapor and sulfur dioxide on the activity of V_2O_5/TiO_2 and CeO_2-V_2O_5/TiO_2 catalysts. 43
CHAPTER V CONCLUSIONS AND RECOMMENDATIONS 47
5.1 Conclusions 47

Page

5.2 Recommendations 47

APPENDICES 50

APPENDIX A 51

CALCULATION FOR CATALYST PREPARATION 51

A1. Calculation for the preparation of V_2O_5/TiO_2 catalyst powder 51

A2. Calculation for the preparation of CeO_2-V_2O_5/TiO_2 catalyst powder 52

APPENDIX B 53

CALCULATION THE RESULT OF ICP-OES 53

APPENDIX C 55

Data of result 55

C1. Data of V_2O_5/TiO2 catalyst on NO conversion 55

C2. Data of CeO_2-V_2O_5/TiO_2 catalyst on NO conversion 56

C3. Data of ammonia oxidation reaction 58

C4. Data of V_2O_5/TiO_2 catalyst on NO conversion at sulfur dioxide condition 60

C5. Data of CeO_2-V_2O_5/TiO_2 catalyst on NO conversion at sulfur dioxide condition 62

C6. Data of V_2O_5/TiO_2 catalyst on NO conversion at water vapor condition 64

C7. Data of CeO_2-V_2O_5/TiO_2 catalyst on NO conversion at water vapor condition 66

C8. Data of V_2O_5/TiO_2 catalyst on NO conversion (Time on stream) at water vapor and sulfur dioxide condition 68

C9. Data of CeO_2-V_2O_5/TiO_2 catalyst on NO conversion (Time on stream) at water vapor and sulfur dioxide condition 69

APPENDIX D 70

Page

CALIBRATING DATA FOR MASS FLOW METER 70
D1. Calibration data of mass flow meter are shown as follows: 70
D1.1 Calibration data of ammonia 71
D1.2. Calibration data of nitrogen oxide 72
D1.3. Calibration data of oxygen 73
D1.4. Calibration data of sulfur dioxide 74
D1.5. Calibration data of nitrogen 75
APPENDIX E 76
DATA OF CALCULATION OF TOTAL ACID SITE 76
APPENDIX F 79
CALCULATION OF THE CRYSTALLITE SIZE 79
REFERENCES 82
VITA 84

LIST OF TABLE

Table **Page**

Table 3.1 The chemicals used in the catalyst preparation. 15

Table 3.2 Compositions of the catalysts prepared for the study 16

Table 3.3 feed gas for catalytic activity measurement 18

Table 4.1 The compositions of metal oxide contained in the catalysts 22

Table 4.2 Specific surface area of catalysts 24

Table 4.3 Amount of acid sites on various of catalyst powders 27

Table C1. Data of V_2O_5/TiO_2 catalyst 55

Table C2. Data of CeO_2-3%V_2O_5/TiO_2 catalyst 56

Table C3. Data of CeO_2-5%V_2O_5/TiO_2 catalyst 57

Table C4. NO Concentration of V_2O_5/TiO_2 catalysts. 58

Table C5. NO Concentration of V_2O_5-CeO_2/TiO_2 catalysts. 59

Table C6. NO conversion of V_2O_5/TiO_2 Catalyst with/without sulfur dioxide in feed gas 61

Table C7. NO concentration (Ammonia oxidation reaction) of V_2O_5/TiO_2 Catalyst with/without sulfur dioxide in feed gas 61

Table C8. NO conversion of CeO_2-V_2O_5/TiO_2 Catalyst with/without sulfur dioxide in feed gas 63

Table C9. NO concentration (Ammonia oxidation reaction) of V_2O_5/TiO_2 Catalyst with/without sulfur dioxide in feed gas 63

Table C10. NO conversion of V_2O_5/TiO_2 Catalyst with/without water vapor in feed gas 65

Table **Page**

Table C11. NO concentration (Ammonia oxidation reaction) of V_2O_5/TiO_2 Catalyst with/without water vapor in feed gas 65

Table C12. NO conversion of CeO_2-V_2O_5/TiO_2 Catalyst with/without water vapor in feed gas 67

Table C13. NO concentration (Ammonia oxidation reaction) of V_2O_5/TiO_2 Catalyst with/without water vapor in feed gas 67

Table C14. NO conversion (Time on stream) of V_2O_5/TiO_2 Catalyst 68

Table C15. NO conversion (Time on stream) of CeO_2-V_2O_5/TiO_2 Catalyst 69

Table D1. Calibration of ammonia 71

Table D2. Calibration of nitrogen oxide 72

Table D3. Calibration of oxygen 73

Table D4. Calibration of sulfur dioxide 74

Table D5. Calibration of nitrogen 75

Table E1. Data for calculation of total acid site 76

LIST OF FIGURE

Figure **Page**

Figure 2.1 Characteristic diagram for SCR process (Ronald et al., 1999) 7

Figure 2.2 Mechanism of SCR over vanadium catalyst in the present of oxygen. (Inomata et al., 1982) 9

Figure 2.3 Proposed structures for monomeric vanadyl species and polymeric metavanadate species in their dehydrated forms on the surface of V_2O_5/TiO_2 catalysts 10

Figure 3.1 Flow diagram of the reactor system for SCR 19

Figure 4.1 XRD patterns of TiO_2 support and V_2O_5/TiO_2catalysts. 23

Figure 4.2 XRD patterns of TiO_2 support and CeO_2-V_2O_5/TiO_2catalysts. 23

Figure 4.3 NH_3-TPD profiles of the catalyst. 26

Figure 4.4 Effect of Vanadium loading on NO conversion 29

Figure 4.5 Effect of Cerium loading on 3%V_2O_5-TiO_2 catalysts. 31

Figure 4.6 Effect of Cerium loading on 5%V_2O_5-TiO_2 catalysts. 31

Figure 4.7 Comparison of NO conversion over 3V30Ce and 5V30Ce catalysts 32

Figure 4.8 NO Concentration of V_2O_5/TiO_2 catalysts. 33

Figure 4.9 NO Concentration of V_2O_5-CeO_2/TiO_2 catalysts. 34

Figure 4.10 The NO conversion of V_2O_5/TiO2 catalyst and V_2O_5-CeO_2/TiO2 catalyst 35

Figure 4.11 NO Concentration of V_2O_5/TiO2 catalyst and V_2O_5-CeO_2/TiO_2 catalyst 36

Figure 4.12 Effect of sulfur dioxide on NO conversion of V_2O_5/TiO_2 Catalyst 38

Figure 4.13 Effect of sulfur dioxide on NO conversion of CeO_2-V_2O_5/TiO_2 Catalyst 39

Figure 4.14 Effect of sulfur dioxide on ammonia oxidation reaction of V_2O_5-TiO_2 Catalyst 39

Figure 4.15 Effect of sulfur dioxide on ammonia oxidation reaction of CeO_2-V_2O_5/TiO_2 Catalyst 40

Figure 4.16 Effect of water vapor on NO conversion of V_2O_5/TiO_2 Catalyst 41

Figure 4.17 Effect of water vapor on NO conversion of CeO_2-V_2O_5/TiO_2 Catalyst 41

Figure 4.18 Effect of water vapor on Ammonia Oxidation reaction of V_2O_5/TiO_2 Catalyst 42

Figure 4.19 Effect of water vapor on ammonia oxidation reaction of CeO_2-V_2O_5/TiO_2 Catalyst 42

Figure 4.20 Temporal profile of NO conversion over V_2O_5/TiO_2 catalyst under the presence of sulfur dioxide and water vapor 45

Figure 4.21 Temporal profile of NO conversion over CeO_2-V_2O_5/TiO_2 catalyst under the presence of sulfur dioxide and water vapor 46

Figure D1. Calibration curve of ammonia 71

Figure D2. Calibration curve of nitrogen oxide 72

Figure D3. Calibration curve of oxygen 73

Figure D4. Calibration curve of sulfur dioxide 74

Figure D5. Calibration curve of nitrogen 75

Figure E1. The calibration curve of ammonia 78

Figure F.1 The (101) diffraction peak of TiO_2 for calculation of the crystallite size 81

CHAPTER I

INTRODUCTION

Nitrogen oxides (NO_x) remain a major source of air pollution. The majority of NO_x is formed by reaction between nitrogen and oxygen at high temperature. NO_x consist of a mixture of 95% NO and 5% NO_2 which derives transportation and power plants. These undesirable byproducts have to be removed before emitting to the surroundings since they contribute to acid rain, photochemical smog, ozone depletion and green-house effects. At present, selective catalytic reduction (SCR) of NO with NH_3 is one of the most efficient methods for reducing nitrogen oxides emissions from stationary sources (Tong et al., 2001). This process is based on the reduction of NO_x with NH_3 to produce nitrogen and water according to the two main reactions.

$$4NO + 4NH_3 + O_2 \longrightarrow 4N_2 + 6H_2O \qquad (1.1)$$

$$2NO_2 + 4NH_3 + O_2 \longrightarrow 3N_2 + 6H_2O \qquad (1.2)$$

During the SCR reactions, when the temperature of SCR reaction exceeds 350°C, NH_3 is partially oxidized by oxygen, instead of NO, according to the following reactions. (Ronald et al., 1999)

$$4NH_3 + 5O_2 \longrightarrow 4NO + 6H_2O \qquad (1.3)$$

$$2NH_3 + 2O_2 \longrightarrow N_2O + 3H_2O \qquad (1.4)$$

$$2NH_3 + 3/2O_2 \longrightarrow N_2 + 3H_2O \qquad (1.5)$$

The oxidation of ammonia consumes the reductant (i.e., ammonia) and lowers the NO_x conversion at high temperature. (Juan et al., 2007) Therefore, the catalyst which possesses high activity in NO elimination may not be the best SCR catalyst because it can give rise to undesirable side reaction. The presence of other components from the emissions of stationary and mobile sources such as H_2O and SO_2 requires further examination of the catalyst activity. The flue gas compositions as well as temperature also vary with the plant due to different kinds of fuel burnt and

operating conditions in each plant. A SCR catalyst designed specifically to the specified flue gas composition and temperature will optimally perform under the design condition.

If sulphur dioxide present in the combustion gas, the oxidation of SO_2 to SO_3 (Equation 1.7) gives rise to the formation of H_2SO_4, resulting in excessive corrosion of process equipment at downstream.

$$2SO_2 + O_2 \longrightarrow 2SO_3 \qquad (1.6)$$

$$SO_3 + H_2O \longrightarrow H_2SO_4 \qquad (1.7)$$

The reaction of NH_3 with SO_3 also results in the formation of NH_4HSO_4 and $(NH_4)_2SO_4$ (Equation 1.8 and 1.9), which deposits on downstream process equipment such as heat exchanger and causes a loss in thermal efficiency.

$$NH_3 + SO_3 + H_2O \longrightarrow NH_4HSO_4 \qquad (1.8)$$

$$NH_3 + SO_3 + H_2O \longrightarrow (NH_4)_2HSO_4 \qquad (1.9)$$

The SCR catalysts should be supported on tinania. In the past, the vanadium catalyst was first found to be active in the SCR process in 1960s. Today, the most commonly used material for this reaction such as V_2O_5, WO_3 and MO_3.

According to previous studies, vanadium oxide catalyst supported on TiO_2 is widely adopted in commercial SCR processes but its activity at low temperature is not very good. CeO_2 has excellent redox properties. Several studies (Zhu at al., 2004) showed that the doping of cerium oxides enhanced the reductivity of the catalyst at low temperature.

The objectives of this research was to study SCR activity of CeO_2 and V_2O_5 supported on titanium dioxide support at low temperature. Moreover, the formation of nitrogen oxide from ammonia oxidation reaction was also investigated.

Previous studies employed V_2O_5- WO_3/ TiO_2 as a SCR catalyst. However, when tungsten precursor was added to washcoat solution, precipitation occurred and the washcoat solution could not be used to coat the catalyst on monolith support. In

this study, cerium was chosen to replace tungsten so as to avoid the problem of precipitation.

The scope of this research is listed as followed.

1. Preparation of TiO_2 support by a sol-gel method

2. Preparation of V_2O_5 on TiO_2 support by an incipient wetness impregnation method. The amount of vanadium in the catalyst ranged from 1 to 7%wt.

3. Addition of CeO_2 over the V_2O_5/TiO_2 catalysts by an incipient wetness impregnation method. The amounts of cerium in the catalyst ranged from 5 to 30%wt.

4. Characterization of catalysts using various techniques

    4.1 Determination of composition of metal by inductively coupled plasma optical emission spectroscopy (ICP-OES)

    4.2 Determination of crystal structure by X-ray diffraction technique (XRD)

    4.3 Determination of specific surface area based on Brunauer, Emmetta and Teller isotherm (BET)

    4.4 Determination of the total acid sites on the catalysts by NH_3 Temperature programmed desorption (NH_3-TPD)

5. Catalytic activity measurement

    5.1 Catalytic activity of SCR reaction

    5.2 Catalytic activity of ammonia oxidation reaction

    5.3 Effect of H_2O and SO_2 on the activity of catalysts

This thesis is organized as followed:

Chapter I introduces the background and motivation of this research.

Chapter II described background information about SCR catalysts.

Chapter III explains procedures for the preparation of support and catalysts, experimental setup and testing procedures.

Chapter IV presents experimental result and discussion of such results.

Chapter V give overall conclusions of this research and recommendations for future research.

CHAPTER II
BACKGROUND INFORMATION

This chapter presents previous studies relate to the selective catalytic reduction of NO by ammonia, side reaction, active phase, reaction mechanism for low temperature selective catalytic reduction of NO_x with NH_3, the effect of water vapor and sulfur dioxide on SCR reaction of NO by NH_3 and literature review about selective catalytic reduction of NO_x by ammonia.

2.1 Nitrogen oxide (Roy et al., 2009, Gomez-Garcia et al., 2005)

Nitrogen oxides (NO, NO_2 and N_2O) emission remains a major air pollutants in flue gas from both automobile and stationary sources. These undesirable byproducts have to be removed before emitting to the surroundings since they contribute to acid rain, photochemical smog, ozone depletion and green-house effects. NO_x is a generic term for nitrogen oxides which are produced during combustion at high temperature according to this reaction.

$$N_2 + O_2 \longrightarrow 2NO \qquad (2.1)$$

$$NO + 1/2O_2 \longrightarrow NO_2 \qquad (2.2)$$

$$2NO \longrightarrow N_2O + 1/2O_2 \qquad (2.3)$$

At ambient temperature, oxygen does not react with nitrogen. However, the producing of NO_x during combustion under high temperature in which it was occurred by combination between nitrogen and oxygen.

2.2 NO_x Formation [Roy et al., 2009]

The major source of nitrogen oxides is the combustion of fossil fuels such as coke in electrical power plants of fossil fuel in the engines of vehicles and aeroplanes. The origin of NO_x is generally categorized into mobile and stationary sources. NO_x is a generic term for nitrogen oxides, namely, NO and NO_2, which are

produced during combustion at high temperature. At ambient temperature, oxygen does not react with nitrogen. However, in an internal combustion engine, high temperature leads to reactions between nitrogen and oxygen to form nitrogen oxides. In the presence of excess oxygen, NO will be converted to NO_2. NO_x from engine exhaust typically consists of a mixture of 95% NO and 5% NO_2.

2.3 Selective catalytic reduction (SCR) of NO by ammonia

Most of NO_x is produced during the combustion process by the oxidation of atmospheric nitrogen at very high temperature. Also NO_x is formed by oxidation of organic nitrogen present in the fuel.

NO_x emissions can be reduced by a variety of methods. The selective catalytic reduction is one of the most widely used technology to reduce nitrogen oxide emissions from stationary sources. This process is based on the reduction of NO_x with NH_3 to produce nitrogen and water according to the two main reactions.

$$4NO + 4NH_3 + O_2 \longrightarrow 4N_2 + 6H_2O \qquad (2.4)$$

$$2NO_2 + 4NH_3 + O_2 \longrightarrow 3N_2 + 6H_2O \qquad (2.5)$$

The reaction between NO and NH_3 can also proceed in a different pathway, leading to the undesired product, N_2O.

$$4NO + 4NH_3 + 3O_2 \longrightarrow 4N_2O + 6H_2O \qquad (2.6)$$

Under typical Selective catalytic reduction condition, equation 2.4 accounts for the overall stoichiometry on the best catalyst. Therefore, ammonia is converted by a pathway other than Equation 2.4. Ammonia can be partially oxidized by oxygen, instead of NO, through one of the following reaction.

$$4NH_3 + 5O_2 \longrightarrow 4NO + 6H_2O \qquad (2.7)$$

$$2NH_3 + 2O_2 \longrightarrow N_2O + 3H_2O \qquad (2.8)$$

$$2NH_3 + 3/2O_2 \longrightarrow N_2 + 3H_2O \qquad (2.9)$$

During the SCR reactions, it is known that when the temperature of the SCR reaction increases above about 350°C, NH_3 reacts with oxygen rather than NO to form nitrogen oxides.

These equations are so-called selective catalytic oxidation (SCO) of ammonia or ammonia oxidation reaction. Several active SCR catalysts are also active in SCO although at a slightly higher temperature. At a temperature below 100-200°C, the ammonia can also react with the NO_x present to produce explosive NH_4NO_3.

$$2NH_3 + 2NO_2 + H_2O \longrightarrow NH_4NO_2 + NH_4NO_3 \quad (2.10)$$

The oxidation of ammonia consumes the reductant (i.e., ammonia) and lowers the NO_x conversion at high temperature. This parallel reaction is described by the characteristic diagram for SCR as shown in Figure 2.1.

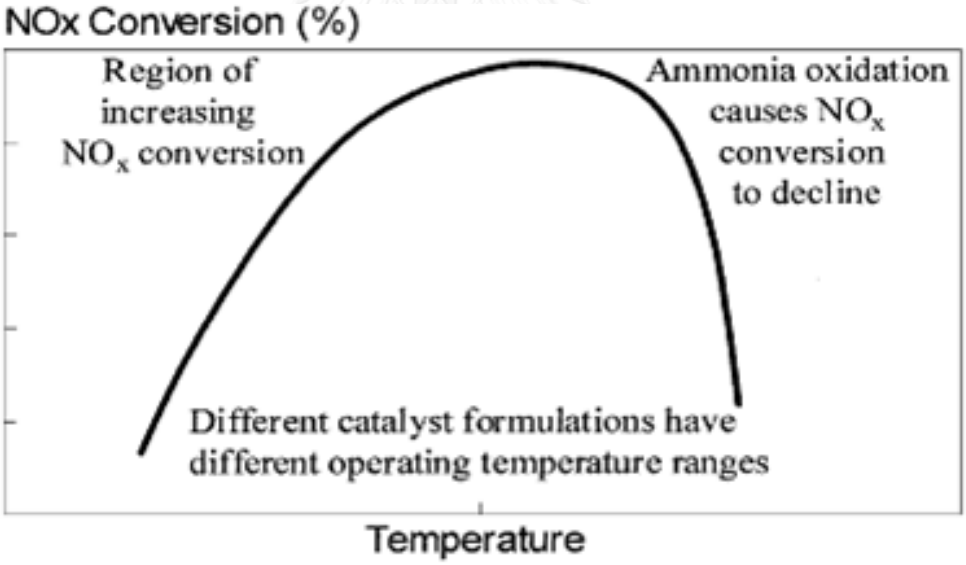

Figure 2.1 Characteristic diagram for SCR process (Ronald et al., 1999)

Therefore, the catalyst which possesses high activity in NO elimination may not be the best SCR catalyst because it can give rise to undesirable side reaction.

When sulphur is present in the flue gas, such as in power plants and petroleum fuel, the oxidation of SO_2 to SO_3 gives rise to the formation of H_2SO_4

(Equation 2.10 and 2.11), resulting in excessive corrosion of process equipment at downstream.

$$2SO_2 + O_2 \longrightarrow 2SO_3 \qquad (2.11)$$

$$SO_3 + H_2O \longrightarrow H_2SO_4 \qquad (2.12)$$

The reaction of NH_3 with SO_3 also results in the formation of NH_4HSO_4 and $(NH_4)_2SO_4$ (Equation 2.13 and 2.14), which deposits on downstream process equipment such as heat exchanger and causes a loss in thermal efficiency.

$$NH_3 + SO_3 + H_2O \longrightarrow NH_4HSO_4 \qquad (2.13)$$

$$NH_3 + SO_3 + H_2O \longrightarrow (NH_4)_2HSO_4 \qquad (2.14)$$

The SCR catalysts should be supported on tinania. In the past, the vanadium catalyst was first found to be active in the SCR process in 1960s. Today, the most commonly used material for this reaction such as V_2O_5, WO_3 and MO_3.

2.4 Mechanism of selective catalytic reduction for V_2O_5-base catalysts **(Busca et al., 1998)**

In figure 2.2, show mechanism of SCR cycle, It was found that the catalytic activity relate with the adsorption of ammonia on the Bronsted acid sites corresponding with V^{5+}-OH sites. V^{5+}=OH groups are also concerned in the reaction, and specifically in the activation of adsorbed ammonia. This activation process implies that transferring of hydrogen from the NH_3 molecule was occurred and then reduced V^{4+}-OH sites were generated. NO from the gas phase reaction can activated ammonia complexes and it can lead to form an intermediate that it can dissociate to nitrogen and water. The oxidation of the reduced V^{4+}-OH sites to V^{5+}=OH groups occurs by gas phase oxygen.

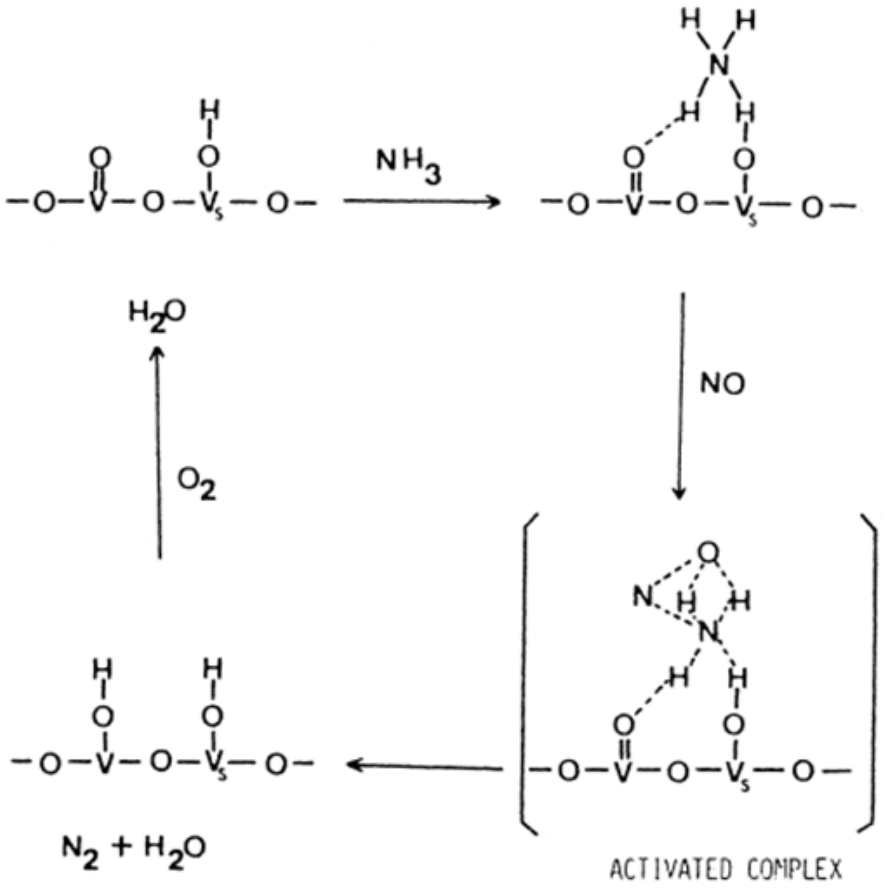

Figure 2.2 Mechanism of SCR over vanadium catalyst in the present of oxygen. (Inomata et al., 1982)

2.5 The active phases and the roles of the support and promoters in the commercial catalysts. (Busca et al., 1998)

Many reports have been published about the characterization of V_2O_5-WO_3/TiO_2 or V_2O_5-MoO_3/TiO_2 model and industrial SCR catalyst. Most studies the appropriated catalyst include monolayer of vanadium and tungsten (or molybdenum) species over the anatase of the TiO_2 support. The amount of metal species such as V_2O_5 in catalyst formulation was need just content in the support. In fact; V_2O_5 is responsible for the activity in the NO_x reduction but in the present of SO_2 the V_2O_5 showed poor catalytic activity due to formulation of undesired oxidation of SO_2 to SO_3 in reaction of gas phase. In very large content of promoter (WO_3, MoO3) can show as inhibitors for the SO_2 oxidation lead to increasing of the

catalyst activity. In the commercial SCR catalyst TiO_2 is used to as a base material to support the active components. The reason of anatase TiO_2 as the best support for SCR catalyst relies on two main reason:

1. SO_2 is usually present in the waste gases of power plants. In the presence of oxygen it can be oxidized to SO_3, thus forming metal sulfate by reacting with the oxide catalyst support. TiO_2 is only weakly and reversibly sulfated in the conditions approaching those of the SCR reaction and the stability of sulfates on the TiO_2. Consequently, TiO_2 based industrial catalysts are only partially and reversibly sulfated at their surfaces upon SCR reaction in the presence of SO_2 and this saltation even enhances the SCR catalytic activity.

2. The supporting V_2O_5 on TiO_2 anatase leads to very active oxidation catalysts and more active than other supports. The reason for this activity enhancement is a result of the good dispersion of vanadium oxide on TiO_2 giving rise to isolated vanadyl centers and polymeric polyvanadate species.

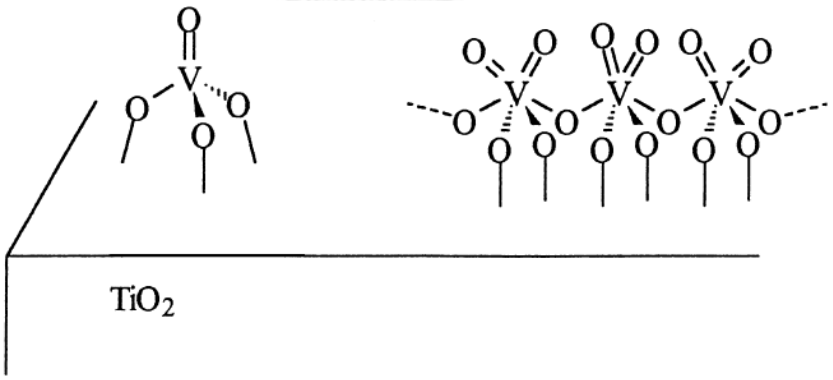

Figure 2.3 Proposed structures for monomeric vanadyl species and polymeric metavanadate species in their dehydrated forms on the surface of V_2O_5/TiO_2 catalysts

Therefore, anatase TiO_2 is an activating support, which was saw that it can resist sulphate species formation, WO_3 and MoO_3 resist both surface area loss of transformation of anatase phase to rutile phase. Another reason for their addition to V_2O_5 supported on TiO_2 is effect of such components in undesired SO_2 oxidation. In

fact, WO_3 and MoO_3 compete with and displace SO_3 on the basic sites of the TiO_2 surface and tend to cover it, thus limiting its sulfation. Therefore, WO_3 and MoO_3 are used as thermal and mechanical stabilizers and as promoter in SCR reaction catalyst.

Pan et al. (2014) studied Effect of support on the performance of Mn–Cu oxides for low temperature selective catalytic reduction of NO with NH_3. The results showed that MnO_x–CuO_x/TiO_2 has better catalytic activity and SO_2 resistance than that of MnO_x–CuO_x/Al_2O3. It could be concluded that support has great impact on the acidity of catalyst.

2.6 The effect of the presence of H_2O and SO_2 on NO reduction

Nova et al. (2000) studied low temperature selective catalytic reduction of NO_x with NH_3 over a TiO_2-supported vanadium–tungsten commercial catalyst and found that the presence of low concentrations of water in the feed stream did not seem to affect the ammonia adsorption–desorption process on the surface but significantly inhibited the SCR reaction. An inhibiting effect of adsorbed NH_3 on the SCR reaction was also pointed out.

Huang et al. (2002) investigated effects of H_2O and SO_2 on V_2O_5/AC catalysts for NO reduction with ammonia at lower temperatures and found that in the absence of SO_2, H_2O inhibited the catalytic activity, which may be attributed to competitive adsorption of H_2O and reactants (NO and/or NH_3). In the absence of H_2O, a small amount of ammonium sulfate salts deposited on the surface of the catalyst, which promoted the SCR activity. However, the deposition rate of ammonium sulfate salts was much greater, which resulted in blocking of the catalyst pores and deactivated the catalyst.

Tang et al. (2007) studied low temperature selective catalytic reduction of NO_x with NH_3 over amorphous MnO_x catalysts. The result indicated that the decrease in activity by H_2O and SO_2 are due to their competing adsorption with the reactant over the catalysts surface. However, most experimental work on the ammonia adsorption has been performed without water in the feed gas. Water has a strong

influence on the ammonia adsorption because it competes with ammonia for the adsorption sites and the activity recovers to the initial level after removing H_2O and SO_2 gases.

Boudali et al. (2009) studied effect of SO_2 oxidation over the WO_3-V_2O_5 supported on sulphated titanium pillared clay catalyst for low temperature selective catalytic reduction of NO_x with NH_3. From this study, it can suggest sulphate stability and reduction properties of SO_4^{2-} or V_2O_5 depended on metal loading in the catalysts. Vanadium increased the catalyst activity of SCR reaction of sulphated Ti-pillared clay. The sulphate species play more important role for catalytic activity of SCR reaction than tungsten species.

How et al. (2009) studied effect of SO_2 oxidation over the V_2O_5/AC catalyst for low temperature selective catalytic reduction of NO_x with NH_3 and reported that the catalyst after SCR reaction in the presence of SO_2 was proved to contain SO_4^{2-} by FT-IR, which indicated that the adsorbed SO_2 over V_2O_5/AC catalyst was in the form of SO_4^{2}, which can increase the surface acidity and ammonia adsorption on the V_2O_5/AC catalyst, and increase the SCR activity.

2.7 Effect of metal oxide for SCR

Chen et al., (1992) reported that the promoter such as WO_3 was commonly added to V_2O_5/TiO_2 catalyst to increase the SCR activity. The promoter preferentially interacted with vanadium oxide species on the titania surface to form two-dimensional surface metal oxide, and then created acid sites on the catalyst surface. The strong interaction between vanadia and tungsten species on the TiO_2 support increased the acidity of TiO_2 and exhibited a higher catalyst activity. WO_3 significantly improved the catalyst activity at a low temperature selective catalytic reduction of NO_x with NH_3 and broadened the temperature window of the maximum NO conversion. The addition of WO_3 also significantly enhanced the resistance of V_2O_5-base catalyst toward alkali metal oxides that are the strongest SCR poisons.

Busca et al., (1998) Vanadium oxide catalyst supported on TiO_2 is widely adopted in commercial SCR processes but its activity at low temperature is not very good.

Media et al., (2002) found that the vanadia content had a major influence on both the SCR activity and the thermal stability. The catalytic activity of 1% V_2O_5 catalysts shows very low results for all cases. For 2% V_2O_5 catalysts, high NO conversion is obtained in new condition and slightly improved after aging procedures 1 (100 h at 550^{o}C) and 2 (100 h at 550^{o}C and 30 h at 600^{o}C). Aging procedure 3 (100 h at 550^{o}C, 30 h at 600^{o}C and 15 h at 650^{o}C) causes the NO conversion of 2% V_2O_5 to decline. The catalytic activity for 3% V_2O_5 catalysts is high in the new condition, and decreases slightly after aging treatments 1, 2. Aging treatment 3 cause the catalytic activity for 3% V_2O_5 to decrease rapidly. The catalyst containing 2% V_2O_5 represents an optimal compromise between the SCR activity and thermal stability over the range of aging treatment. 1% V_2O_5 catalysts results in low SCR activity, and 3% V_2O_5 shows a significant low thermal stability.

XU et al., (2008) studied the selective catalytic reduction of NO_x by NH_3 over a Ce/TiO_2 catalyst. From experiment, catalysts that have Ce Content from 5% to higher value showed high activity in the temperature rang 274-400oC. All the catalyst can resist to SO_2 and H_2O under test condition.

Gao et al., (2010) studied the activity and characterization of Ce/TiO_2 catalysts prepare by the sol-gel method for the selective catalytic reduction of NO_x by NH_3. From experiment, it showed that catalyst activity increased significantly after Ce was added. NO_x conversion increased with Ce loading up 0.6 of mass ratio of Ce/TiO_2. In the present of H_2O and SO_2, the SCR of NO with NH_3 over the catalyst was increased with the reaction temperature.

Liu et al., (2014) studied the addition of MoO_3 enhanced the activity of CeO_2/TiO_2 catalyst for the selective reduction of NO_x with NH_3. The MoO_3-promoted CeO_2/TiO_2 exhibited higher activity than CeO_2/TiO_2 even in the co-presence of H_2O and SO_2. This is because the introduction of Mo to the $10CeO_2/TiO_2$ catalyst can

inhibit the adsorption of H_2O and SO_2 as well as the formation of sulfate species on the catalyst surface, thus alleviating the poisoning effect of H_2O and SO_2.

CHAPTER III
EXPERIMENTAL

This chapter describes preparation methods for V_2O_5/TiO_2 and V_2O_5-CeO_2/TiO_2 catalyst powder, catalyst characterization and activity testing system.

3.1. Catalyst preparation

3.1.1 Chemicals

All chemicals used in this research are listed in Table 3.1

Table 3.1 The chemicals used in the catalyst preparation.

Chemical	Supplier
Titanium (IV) isopropoxide	Aldrich
Ammonium metavanadate, 99.99%	Aldrich
Cerium(III) nitrate hexahydrate, 99.99%	Aldrich
Oxalic acid hydrate	Fluka

3.1.2 Preparation of V_2O_5/TiO_2 and V_2O_5-CeO_2/TiO_2 catalyst powder

Titania support was prepared by a sol-gel method using titanium isopropoxide as precursor. Firstly, 83.5 ml of titanium isopropoxide was dissolved with 7.51 ml of nitric acid 65% in 1000 ml of de-ionized water. Then the mixture was stirred for 3 days. The obtained clear sol was dialyzed by cellulose membrane in de-ionized water in order to adjust pH to be 3.5. The obtained dialyzed titania sol was dried at 110°C for 16 hours, crushed, and then calcined at 350°C for 2 hours. The vanadium catalyst (V_2O_5/TiO_2) was prepared by impregnating TiO_2 with a proper amount of ammonium metavanadate (NH_4VO_3) and oxalic acid solution, then dried at 110°C for 16 hours and calcined at 500°C for 2 hours in air. Cerium and vanadium catalysts (V_2O_5-CeO_2/TiO_2) were prepared by the same method as described above by using

cerium nitrate as a precursor for Ce. Cerium nitrate was dissolved separately in distilled water and impregnated in vanadium catalyst, then dried at 110°C for 16 hours and calcined at 500°C for 2 hours in air. The composition of the catalysts were listed in table 3.2.

Table 3.2 Compositions of the catalysts prepared for the study

Sample	Symbol	Content (%wt)	
		V_2O_5	CeO_2
1%V_2O_5/TiO_2	1V	1	-
3%V_2O_5/TiO_2	3V	3	-
5%V_2O_5/TiO_2	5V	5	-
7%V_2O_5/TiO_2	7V	7	-
3%V_2O_5-5%CeO_2/TiO_2	3V5Ce	3	5
3%V_2O_5-10%CeO_2/TiO_2	3V10Ce	3	10
3%V_2O_5-20%CeO_2/TiO_2	3V20Ce	3	20
3%V_2O_5-30%CeO_2/TiO_2	3V30Ce	3	30
5%V_2O_5-5%CeO_2/TiO_2	5V5Ce	5	5
5%V_2O_5-10%CeO_2/TiO_2	5V10Ce	5	10
5%V_2O_5-20%CeO_2/TiO_2	5V20Ce	5	20
5%V_2O_5-30%CeO_2/TiO_2	5V30Ce	5	30

3.2 Characterization of catalyst

3.2.1 Surface area measurement

The specific surface area was determined by nitrogen adsorption method. The specific surface area of the catalysts was measured by Micrometrics ChemiSorb 2750 using nitrogen as the adsorbate. The amount of the catalyst used was 0.1 g. The sample was degassed at 200°C prior to each measurement.

3.2.2 X-ray diffraction (XRD)

The X-ray diffraction patterns of the catalysts were performed by using a BRUKER D8 ADVANCE X-ray diffractrometer with CuKα radiation (λ=0.154056 nm) in the 2θ range of 20-80°. The XRD spectrum is used to identify the crystal structure of the catalyst.

3.2.3 Inductively Coupled Plasma-Optical Emission Spectroscopy (ICP-OES)

The amount of metal deposited on the surface of titanium dioxide (TiO_2) was measured with an Optima 2100 DV spectrometer. A powder of catalyst was digested into solution phase. Firstly, we dissolved 0.01 g of catalyst 7 ml of 97% H_2SO_4 acid (Sigma Aldrich). Next, 2.7 g of $(NH_4)_2SO_4$ was added into solution while being stirred until homogeneous solution was obtained. Then the resulting solution was made up to 100 ml with deionized water. The solution is ready to measure and compare with a calibration curve to obtain an amount of metal loading.

3.2.4 NH_3 temperature program desorption (NH_3-TPD)

The temperature program desorption (TPD) using NH_3 as a probe molecule was performed in a Micrometric ChemiSorb 2750 automated system attached with ChemiSoft software. The amount of NH_3 adsorbed on the surface was determined by thermal conductivity detector.

The catalyst sample, approximately 0.1g of sample was placed in glass tube in a temperature-controlled furnace. Helium gas with a flow rate 25 ml/min was fed through sample. The sample was heated from a room temperature to 500 ℃ with a heating rate of 10 ℃/min and held for one hour to remove moisture. Then the sample was cooled down to 100 ℃. After that, 15%vol of NH_3 in helium gas was flowed through sample at a flow rate of 25 ml/min and held for 30 minutes. Subsequently, helium gas was flowed through sample at flow rate of 25 ml/min for 45 minutes. Finally, the sample was heated from a room temperature to 500 ℃ with a heating rate of 10 ℃/min. The signal from this step was recorded every one second and stored on a microcomputer.

3.3 Catalytic activity measurement

All feed gas for catalytic activity measurement are listed in Table 3.3

Table 3.3 feed gas for catalytic activity measurement

Feed gas	Supplier
He (99.999%)	Linde
Air Zero (Zero grade)	Linde
NH_3 (10000 ppm in N_2)	BOC Scientific
SO_2 (10000 ppm in N_2)	BOC Scientific
NO (10000 ppm in N_2)	BOC Scientific
N_2 (99.999%)	Linde
O_2 (>=99.9%)	Linde

The reactor used is a 7 mm ID stainless tubular fixed bed reactor. An electric furnace is used to supply heat to the reactor. Temperature of the furnace is controlled by a digital temperature controller. The diagram of the system is exhibited schematically in Figure 3.1. The feed gas mixture contained 120ppm NO, 120ppm NH_3, 30ppm SO_2 and 15%vol H_2O. The concentration of O_2 was 15% by volume. And the rest was balanced with N_2. In case of ammonia oxidation study, NO gas was removed from the feed gas mixture. The total flow rate of feed gas mixture was 200 ml/min. The flow of each feed gas stream was controlled by mass flow controllers. The temperature was varied in the range of 120-450°C. In each run about 0.1 g of the prepared catalyst is tested by passing the feed gas stream through the catalyst bed packed on quartz wool. NO concentration in outlet stream was measured by gas chromatography. NO conversion is calculated from the following equation (3.1). No concentration is analyzed using a gas chromatograph Shimadzu GC-2014

$$\text{NO conversion}(\%) = \frac{\text{NO}_{\text{in}} - \text{NO}_{\text{out}}}{\text{NO}_{\text{in}}} \times 100 \qquad (3.1)$$

Reaction condition for catalyst activity testing system

Reaction temperature	120-450	°C
Operation pressure	1	atm

Component of feed gas mixture:

Nitrogen oxide	120	ppm
Ammonia	30	ppm
Water vapor	15	%vol (when used)
Sulfur dioxide	30	ppm (when used)
Nitrogen	balance	

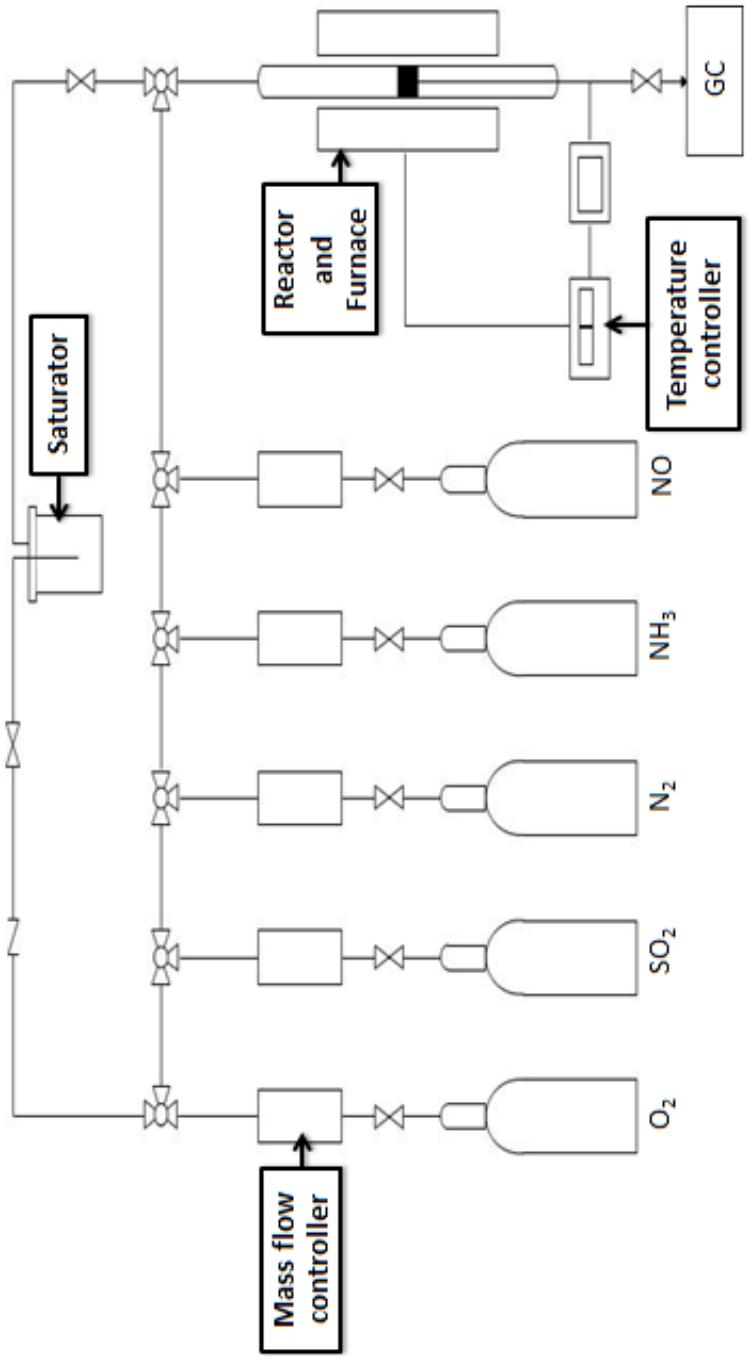

Figure 3.1 Flow diagram of the reactor system for SCR

CHAPTER IV
RESULTS AND DISCUSSION

In this chapter presents the results of selective catalytic reduction of nitrogen oxide by ammonia over CeO_2-V_2O_5-TiO_2 catalysts are reported. The results and discussions are divided into four main parts. The first part, section 4.1, discusses the results of the various characterization techniques for catalyst properties of CeO_2 in V_2O_5-TiO_2 catalyst. The second part, section 4.2, discusses about activity of catalysts for low-temperature selective catalytic reduction of nitrogen oxide by ammonia. The third part, section 4.3, discusses about the formation of nitrogen oxide from ammonia oxidation reaction. The final part, section 4.4, discusses activity of V_2O_5-TiO_2 and CeO_2-V_2O_5-TiO_2 catalysts in the present of water vapor and sulfur dioxide conditions.

4.1 Characterization of V_2O_5-TiO_2 and CeO_2-V_2O_5-TiO_2 catalysts

In this section, present the results from characterization of V_2O_5-TiO_2 and CeO_2-V_2O_5-TiO_2 catalysts. The catalysts are characterized by inductively coupled plasma-optical emission spectroscopy (ICP-OES) to determine the percentage of metal loading of each catalyst. XRD to determine crystal structure patterns of the catalyst. The specific surface area was determined by nitrogen adsorption method. NH_3-TPD to determine amounts of total acid site on the catalyst surface.

4.1.1 Composition of metal oxide contained in the catalyst

The amounts of vanadium oxide (V_2O_5) and cerium oxide (CeO_2) in the catalyst were determined by ICP-OES. The compositions of the catalysts are shown in table 4.1. From the results, the actual contents of both V_2O_5 and CeO_2 were comparable to the intended contents of both oxides from preparation. The calculation of compositions of metal oxide contained in the catalysts as shown in Appendix B.

Table 4.1 The compositions of metal oxides contained in the catalysts

Catalyst	V_2O_5 Content (%wt)		CeO_2 Content (%wt)	
	Intended	Actual	Intended	Actual
1V	1	0.93	-	-
3V	3	2.71	-	-
5V	5	4.31	-	-
7V	7	6.57	-	-
3V5Ce	3	2.57	5	4.92
3V10Ce	3	2.99	10	8.82
3V20Ce	3	3.04	20	18.50
3V30Ce	3	2.62	30	27.66
5V5Ce	5	5.11	5	4.82
5V10Ce	5	4.34	10	8.51
5V20Ce	5	4.47	20	18.15
5V30Ce	5	4.10	30	28.55

4.1.2 X-ray diffraction (XRD)

Bulk crystal structure and phase of a crystalline material can be detected by diffraction of an X-ray beam as a function of angle of the incident beam. XRD patterns of catalysts are shown in Figures 4.1 and 4.2. XRD result indicated that all catalyst powder consisted of anatase phase of TiO_2 according to the peaks at 2Theta of 25.4°, 38.2°, 48.2°, 54.3°, 63.2°, and 75.4°. The amount of rutile and brookite phase was also detected in every sample.

Since no peak was observed for V_2O_5 or CeO_2 compounds, vanadium and cerium were believed to be well dispersed over the samples or were in too small of a loading. In case CeO_2 be able to from amorphous phase. The amount of rutile phase decreases with an increase in vanadium loading (Figures 4.1 and 4.2).

TiO_2 in anatase phase was a suitable carrier for SCR catalyst (Zhu et al., 2004). Therefore, the presence of anatase phase in vanadium catalyst is helpful to enhance

its SCR activity. The addition of V_2O_5 leads to transformation of rutile to anatase phase. (Busca et al., 1998)

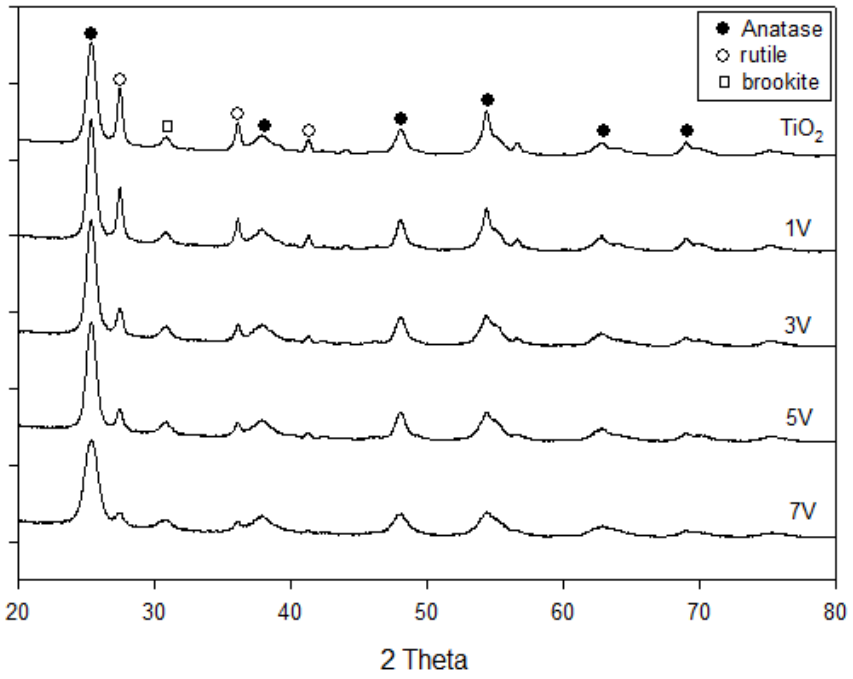

Figure 4.1 XRD patterns of TiO_2 support and V_2O_5/TiO_2catalysts.

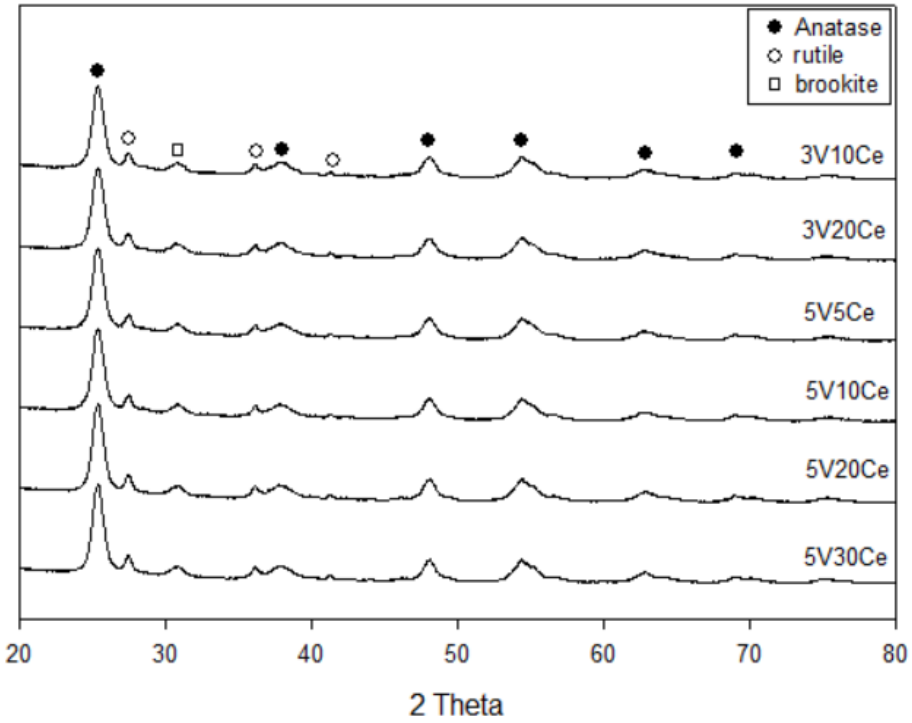

Figure 4.2 XRD patterns of TiO_2 support and CeO_2-V_2O_5/TiO_2catalysts.

4.1.3 Specific surface area and crystallite size of the catalysts

The specific surface area was determined by nitrogen adsorption method. The single point BET specific surface area of the catalyst was measured by Micrometric ChemiSorb 2750 using nitrogen as the adsorbate. BET specific area of the catalysts is listed in table 4.2.

Table 4.2 Specific surface area of catalysts

Catalyst	BET/$m^2 \cdot g^{-1}$	Crystallite size (nm)[a]
TiO_2	88.04	7.977
1V	56.04	9.102
3V	59.96	11.354
5V	58.99	13.526
7V	49.21	14.254
3V5Ce	60.51	6.852
3V10Ce	61.85	6.789
3V20Ce	64.14	6.524
3V30Ce	66.87	6.214
5V5Ce	64.05	6.698
5V10Ce	65.48	6.585
5V20Ce	69.11	6.012
5V30Ce	74.32	5.325

[a] Calculated by Debye-Scherrer equation from XRD spectra Appendix F.

The crystallite sizes of anatase TiO_2 in the catalyst and specific surface areas were also showed in Table 4.2 The specific surface areas of the SCR catalysts are lower than that of titania (88.04 m^2/g), possibly due to the SCR catalysts are calcined several times. The specific surface areas of V_2O_5 /TiO_2 catalysts decreased progressively from 56.04 to 49.21 m^2/g, with increasing V_2O_5 content from 1 to 7 %wt. V_2O_5. This is possibly due to the formed V_2O_5 block some pore of the support of catalyst.

The increasing amount of vanadium loading lowered the specific surface area of the catalyst, compared with that of pure titania support. The crystallite sizes of titania in the catalyst became slightly larger and were 7.977 nm. The crystallite size was calculated from XRD peak width using Debye-Scherrer equation as shown in Appendix F. The crystallite size grew larger when vanadium was added.

The specific surface areas of V_2O_5-CeO_2/TiO_2 catalysts also shown in Table 4.2. The specific surface areas of catalyst was larger than that of V_2O_5/TiO_2 catalyst. At 3%V_2O_5-CeO_2/TiO_2 catalysts, the specific surface areas increased progressively from 60.51 to 66.87 m^2/g with increasing CeO_2 content from 5 to 30 %wt.. And 5%V_2O_5-CeO_2/TiO_2 catalysts, the specific surface areas also increased progressively from 64.05 to 74.35 m^2/g with increasing CeO_2 content from 5 to 30 %wt.

The crystallite sizes of V_2O_5-CeO_2/TiO_2 catalyst became slightly lower then V_2O_5/TiO_2 catalyst. The crystallite size was calculated from XRD peak width using Debye-Scherrer equation as shown in Appendix F. The crystallite size grew smaller when cerium was added. The specific surface area increased after the cerium was loaded on the V_2O_5/TiO_2 catalyst because some cerium oxide could inhibit the agglomeration of the TiO_2 crystallited.

According to Xu et al., (2001), the specific surface area of CeO_2/TiO_2 catalysts increases because some cerium can inhibit the agglomeration of the TiO_2 crystallites and the specific surface area of pure CeO_2 is 90.5 m^2/g (pure TiO_2). The increasing of CeO_2 in TiO_2, the overall specific surface area will be increased.

The 5V30Ce catalyst that exhibits the largest surface area in the series. This finding suggests that the BET surface area is one of the factors affecting SCR activities of the V_2O_5-CeO_2/TiO_2 catalysts with different Ce contents.

4.1.4 Concentration of acid site of catalyst

Temperature program desorption (TPD) using NH_3 as a probe molecule was performed in a Micrometric ChemiSorb 2750 automated system attached with

ChemiSoft software. The amount of NH_3 adsorbed on the surface was determined by thermal conductivity detector.

Temperature program desorption of ammonia is a commonly used technique for determination of amount and strength of surface acid sites. Desorption temperature of ammonia can be qualitatively related to the corresponding the strength of the acid site. And the amount of the acid sites can be quantitatively determined from the amount of NH_3 which adsorbed on the sample. From NH_3-TPD results, the amounts of acid sites were calculated from the area under the curve and listed in Table 4.3.

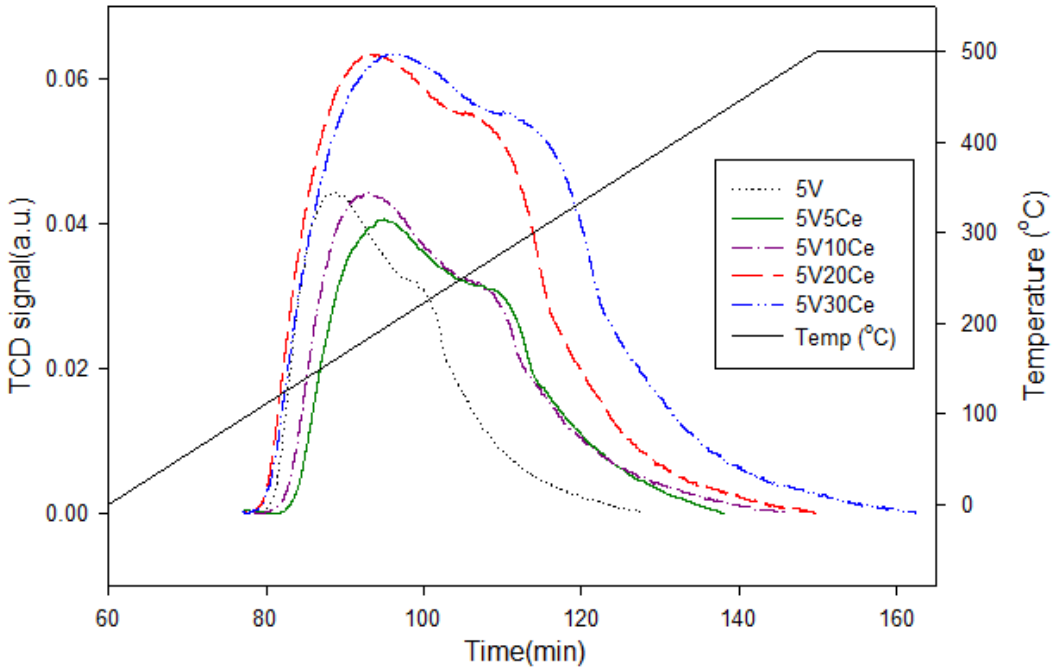

Figure 4.3 NH_3-TPD profiles of the catalyst.

From figure 4.3 displays the result of NH_3-TPD. For the catalysts the adsorption occurred between 150 and 500 $^{\circ}$C. The amount of total acid site was calculated from area under the curve and was listed in Table 4.3. The calculation of total acid site of catalyst as shown in Appendix E.

The addition of CeO_2 in V_2O_5/TiO_2 catalyst increased the amount of acid site in catalyst progressively from 1.019 to 2.054 mmol NH_3/g with increasing CeO_2 content from 5 to 30 %wt.., which could be attributed to its higher SCR performance.

According to NH_3-TPD results, the increasing of acidity was beneficial for selective catalytic reduction of NO by NH_3 (Busca et al., 1998)

Table 4.3 Amount of acid sites on various of catalyst powders

Catalyst	Total acid site (mmol NH_3/g)
5V	1.019
5V5Ce	1.197
5V10Ce	1.431
5V20Ce	1.936
5V30Ce	2.054

4.2 Selective catalytic reduction of NO by NH_3 over V_2O_5-TiO_2 and CeO_2-V_2O_5/TiO_2 catalysts

This section shows the catalytic activities of the catalysts. The results are divided into two main parts. The first part, section 4.2.1, presents the catalytic activities of V_2O_5/TiO_2 catalysts by various loading metal oxides. The second part, section 4.2.2, presents the catalytic activities of CeO_2-doped in V_2O_5/TiO_2 catalyst for low-temperature selective catalytic reduction of nitrogen oxide by ammonia by various loading metal oxides.

The activity measurements were carried out in a fixed-bed reactor using 0.1 g of powder catalyst. The experimental setup is displayed in Figure 3.1. The feed gas mixture contained 120ppm NO, 120ppm NH_3. The concentration of O_2 was 15% by volume. And the rest was balanced with N_2.

4.2.1 Activity of V_2O_5/TiO_2 catalysts

The results of selective catalytic reduction of NO by NH_3 over V_2O_5/TiO_2 catalyst powder with various compositions of vanadium in the reaction temperature range of 120-450°C. The composition of feed gas mixture contained 120ppm NO, 120ppm NH_3. The concentration of O_2 was 15% by volume. And the rest was balanced with N_2.

The effect of V_2O_5 loading on NO conversion over V_2O_5/TiO_2 catalyst at 1, 3, 5, and 7 %wt is shown in Figure 4.4. SCR activities of the catalysts increase with increase with temperature to 250°C and SCR activities of the catalysts decrease at temperature above 350 °C by ammonia oxidation reaction (Figure 4.8); During the SCR reactions, it is known that when the temperature of the SCR reaction increases above about 350°C, NH_3 reacts with oxygen rather than NO to form nitrogen oxides. Several active SCR catalysts are also active in SCO although at a slightly higher temperature.

Moreover, 3V and 5V catalysts exhibited the high catalytic activity with provide 78% and 85% NO conversion, respectively, at the temperature 250°C. The catalysts with 3% and 5%wt V_2O_5 loading possessed the best SCR activities because of high specific surface areas 59.96 and 58.99 m^2/g and were selected for in subsequent studies.

At low temperature the NO conversion increase with increase V_2O_5 content because V_2O_5 is active site exhibit an appreciable activity in the SCR reaction. (Lietti et al., 2000)

At 7V catalyst, SCR activities of the catalysts decreased with increase vanadium loading. This is possibly due to the formed V_2O_5 block some pore of the support of catalyst. Moreover, 7V catalyst exhibited lower catalytic activity than 3V and 5V catalyst.

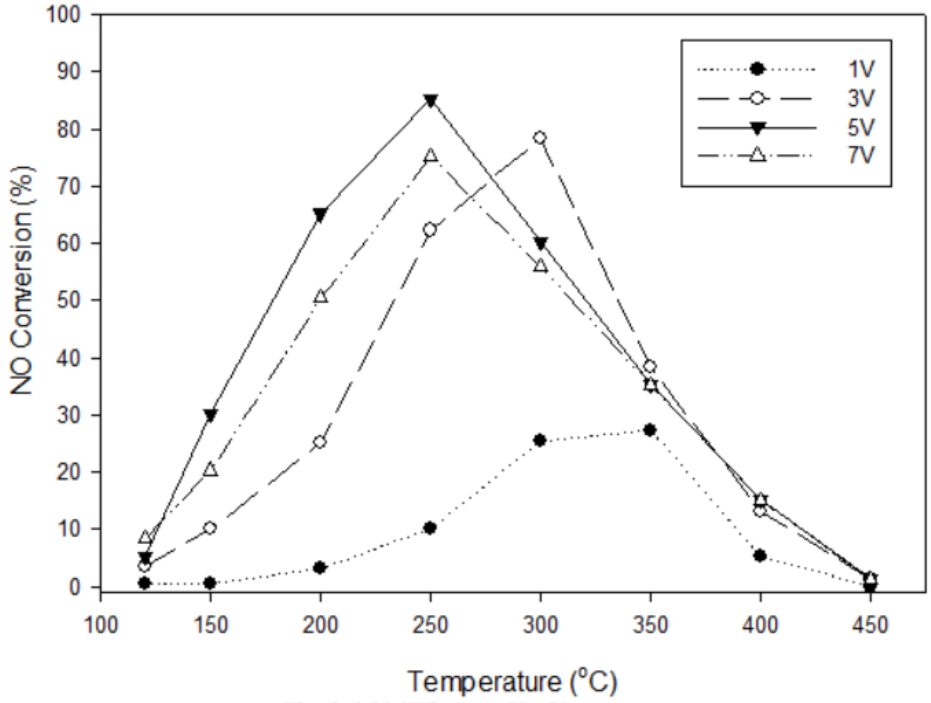

Figure 4.4 Effect of Vanadium loading on NO conversion

4.2.2 Effect of CeO_2 on the activity of V_2O_5/TiO_2 catalyst

The results of Selective catalytic reduction of NO by NH_3 over CeO_2-V_2O_5/TiO_2 catalyst powder with various compositions of vanadium in the reaction temperature range of 120-450°C. The composition of feed gas mixture contained 120ppm NO, 120ppm NH_3. The concentration of O_2 was 15% by volume. And the rest was balanced with N_2.

The effect of CeO_2 loading on NO conversion over V_2O_5/TiO_2 catalyst at 5, 10, 20, and 30 %wt is shown in Figure 4.5 and 4.6. SCR activities of the catalysts increased with increase CeO_2 content and increase with temperature to 250°C. The SCR activities of the catalysts decreased at temperature above 350°C by ammonia oxidation reaction (Figure4.9).; During the SCR reactions, it is known that when the temperature of the SCR reaction increases above about 350°C, NH_3 reacts with oxygen rather than NO to form nitrogen oxides. Several active SCR catalysts are also active in SCO although at a slightly higher temperature

Figure4.5 shows the catalytic activity of 3%V_2O_5-CeO_2/TiO_2 catalysts with various compositions of cerium at 0, 5, 10, 20 and 30 %wt., the catalytic activity at temperature 300^{o}C increased progressively 78.96, 80.32, 85.63, 88.53 and 90.63 %NO conversion, respectively.

Figure4.6 shows the catalytic activity of 5%V_2O_5-CeO_2/TiO_2 catalysts with various compositions of cerium at 0, 5, 10, 20 and 30 %wt., the catalytic activity at temperature 250^{o}C increased progressively 85.18, 90.37, 92.13, 95.25 and 100 %NO conversion, respectively.

Moreover, 3V30Ce and 5V30Ce catalysts exhibited the high catalytic activity with provide 90.63% and 100% NO conversion, respectively. The 3V30Ce and 5V30Ce catalysts possessed the best SCR activities.

Figure 4.7 showed the comparison of 3V30Ce and 5V30Ce catalysts. The catalysts provide 90.63% and 100% NO conversion at temperature 250 and 300^{o}C, respectively. The 5V30Ce catalyst exhibit superior activity especially at lower temperature. To elucidate the the addition of CeO_2 increased the catalyst surface area (table 4.2) and the total acid site of catalyst (Table 4.3), leading to high catalytic activity were shown in following part 4.2.

According to Gao et al., (2004) the activity and characterization of CeO_2/TiO_2 catalysts prepare by the sol-gel method for the selective catalytic reduction of NO_x by NH_3. From experiment, it showed that catalyst activity increased significantly after Ce was added. The result shown 20% Ce/TiO2 catalyst that showed the best SCR activity has the largest surface area in this series, which suggests that the appropriate cerium loading. This finding indicates that the BET area is one of the main reasons for the different catalytic activities of the Ce/TiO2 catalysts with different Ce contents.

According to XU et al., (2008) studied the selective catalytic reduction of NO_x by NH_3 over a CeO_2/TiO_2 catalyst. From experiment, catalysts that have Ce Content from 5% to higher value showed high activity in the temperature rang 274-400^{o}C. The result shown that the addition of CeO_2 increased the catalyst surface area lead to high catalyst activity at low temperature.

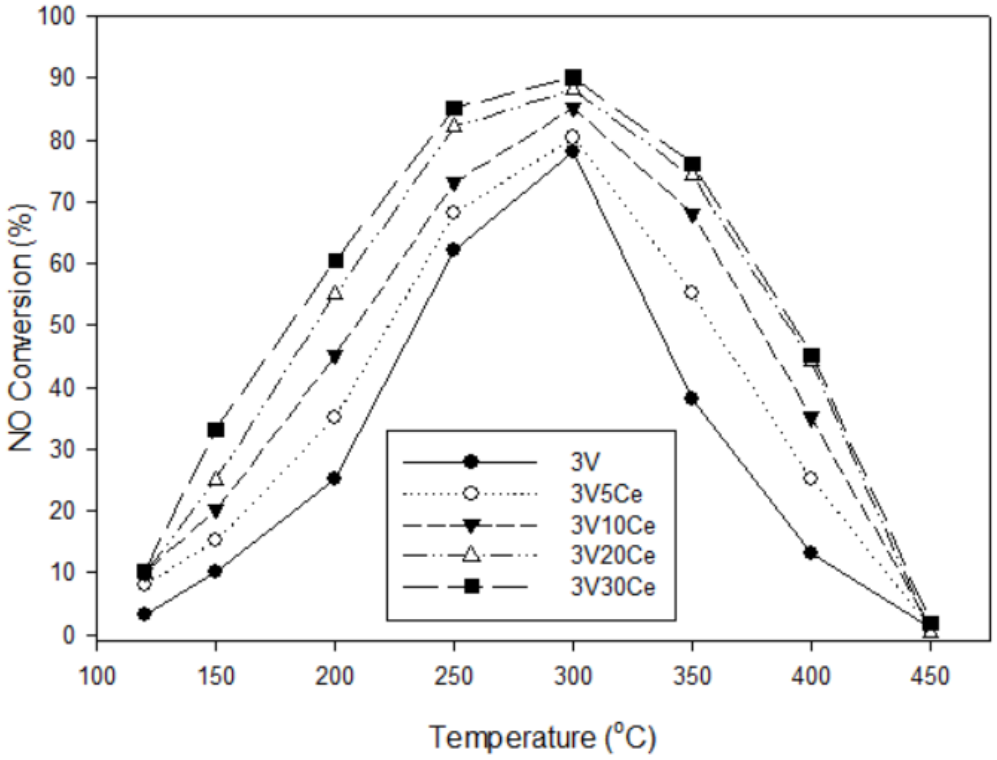

Figure 4.5 Effect of Cerium loading on 3%V_2O_5-TiO_2 catalysts.

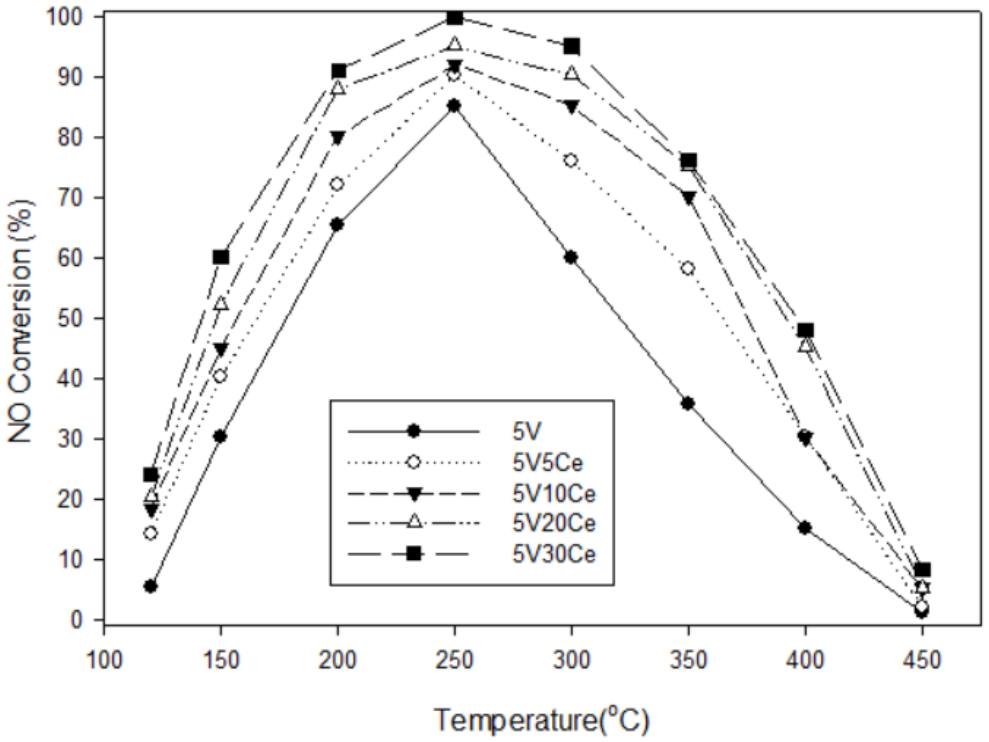

Figure 4.6 Effect of Cerium loading on 5%V_2O_5-TiO_2 catalysts.

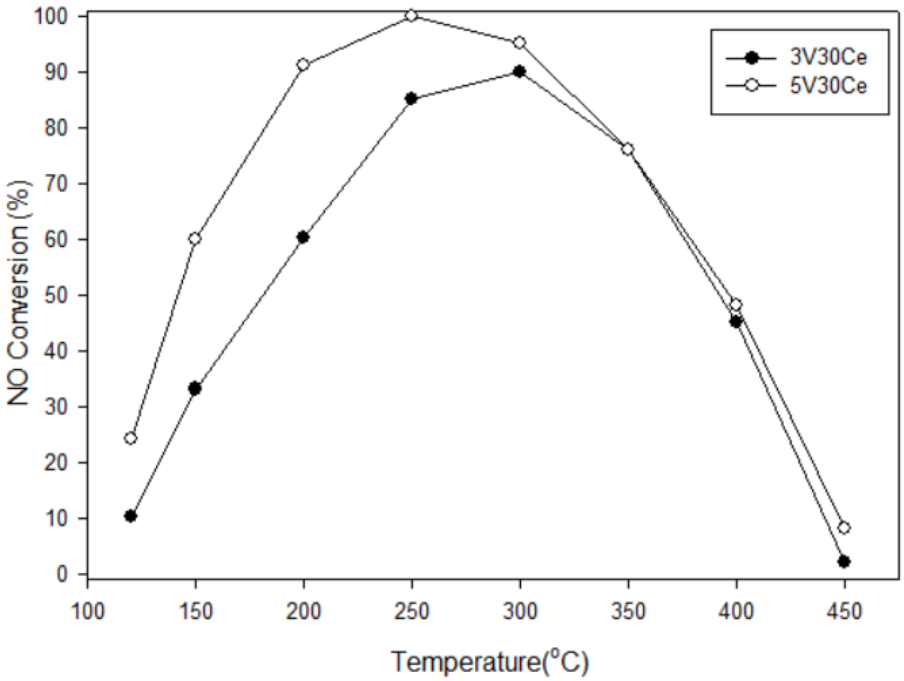

Figure 4.7 Comparison of NO conversion over 3V30Ce and 5V30Ce catalysts.

4.3 The formation of nitrogen oxide from ammonia oxidation reaction.

In this part, we discusses about the formation of nitrogen oxide from ammonia oxidation reaction (Equation 1.3-1.5). The feed gas mixture contained 120 ppm NH_3. The concentration of O_2 was 15% by volume. And the rest was balanced with N_2. In case of ammonia oxidation study, NO gas was removed from the feed gas mixture. The total flow rate of feed gas mixture was 200 ml/min.

The selective catalytic reduction (SCR) of NO with NH_3. This process is based on the reduction of NO_x with NH_3 to produce nitrogen and water according to the two main reactions.

$$4NO + 4NH_3 + O_2 \longrightarrow 4N_2 + 6H_2O \qquad (1.1)$$

$$2NO_2 + 4NH_3 + O_2 \longrightarrow 3N_2 + 6H_2O \qquad (1.2)$$

During the SCR reactions, when the temperature of SCR reaction exceeds 350°C, NH_3 is partially oxidized by oxygen, instead of NO, according to the following reactions. (Ronald et al., 1999)

$$4NH_3 + 5O_2 \longrightarrow 4NO + 6H_2O \qquad (1.3)$$

$$2NH_3 + 2O_2 \longrightarrow N_2O + 3H_2O \qquad (1.4)$$

$$2NH_3 + 3/2O_2 \longrightarrow N_2 + 3H_2O \qquad (1.5)$$

The oxidation of ammonia consumes the reductant (i.e., ammonia) and lowers the NO_x conversion at high temperature. (Juan et al., 2007) Therefore, the catalyst which possesses high activity in NO elimination may not be the best SCR catalyst because it can give rise to undesirable side reaction.

In order to determine the catalyst behavior in the ammonia oxidation process, a series of experiments between 250 to 450°C was carried out and the results shown in Figures 4.8 and 4.9.

The results of ammonia oxidation reaction over V_2O_5-TiO_2 catalyst powder with various compositions of vanadium at 1, 3, 5, and 7 %wt. As vanadium loading increased, the concentration of NO at 450°C (product of ammonia oxidation) increased 35, 41, 68, 75 ppm, respectively. From the experiment (Figure 4.8), ammonia oxidation appeared to happen at a temperature greater than 350°C and the extent increased with temperature.

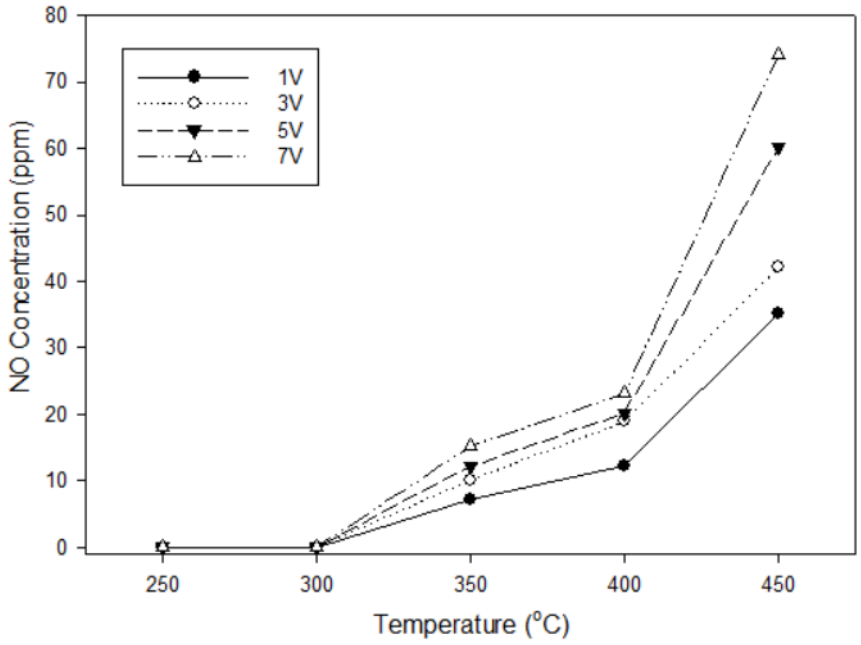

Figure 4.8 NO Concentration of V_2O_5/TiO_2 catalysts.

The concentration of NO increase because vanadium is an active catalyst, which also catalyzes ammonia oxidation reaction at high temperature than main reaction (SCR reaction).

The oxidation of ammonia consumes the reductant (i.e., ammonia) and lowers the NO_x conversion at high temperature. (Busca et al., 1998)

NH_3 is partially oxidized by oxygen, instead of NO, according to the following reactions (Equation 1.3). (Ronald et al., 1999)

$$4NH_3 + 5O_2 \longrightarrow 4NO + 6H_2O \qquad (1.3)$$

The result of ammonia oxidation over V_2O_5-CeO_2/TiO_2 catalyst powder with various compositions of cerium at 5, 10, 20, and 30 %wt. is shown in Figure 4.8. NO was detected at 400 and 450°C, the concentration of NO at 450°C (product of ammonia oxidation) is 42, 35, 30, 18 ppm, respectively. The extent of ammonia oxidation decreased with increasing cerium loading.

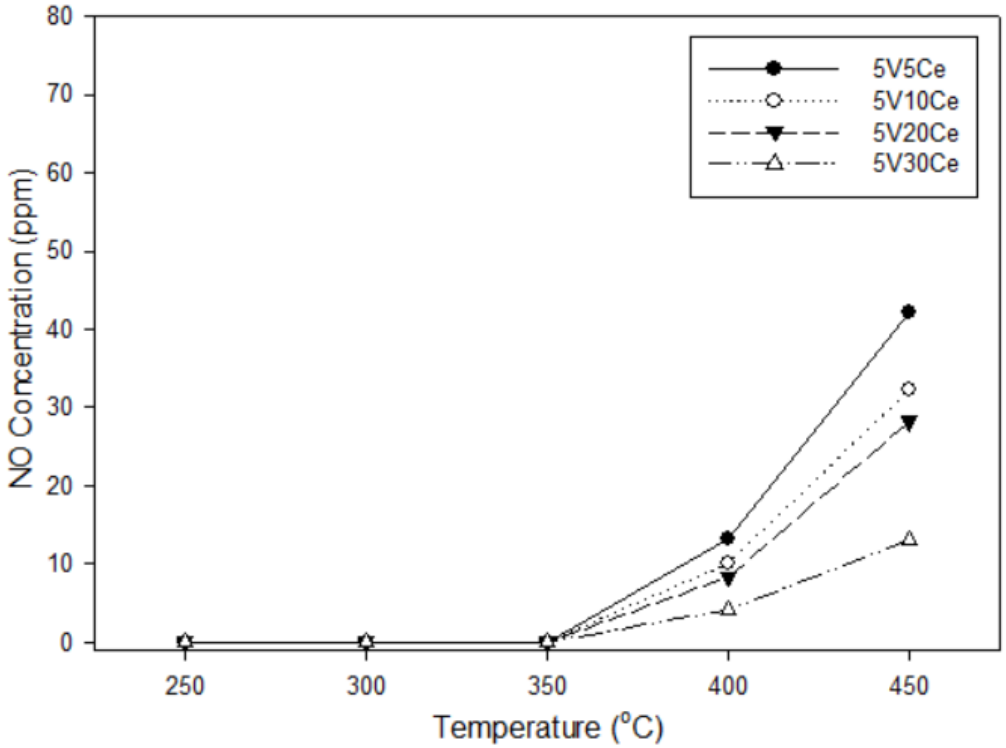

Figure 4.9 NO Concentration of V_2O_5-CeO_2/TiO_2 catalysts.

The addition of cerium to the catalyst inhibited ammonia oxidation reaction, retained the SCR activity at high temperature and broadened the temperature window of the maximum NO conversion.

Figure 4.10 showed the comparison of V_2O_5 /TiO_2 catalyst and V_2O_5-CeO_2/TiO_2 catalyst. At high temperature, the NO conversion increase with increase CeO_2 content because the addition of CeO_2 decreased the effect of the ammonia oxidation. At temperature 450 $^{\circ}C$ the concentration of NO (Figure4.11) (product of ammonia oxidation) of V_2O_5-CeO_2/TiO2 catalyst (18 ppm) compared with V_2O_5/TiO_2 catalyst (68 ppm), the addition of cerium to the catalyst inhibited ammonia oxidation effect.

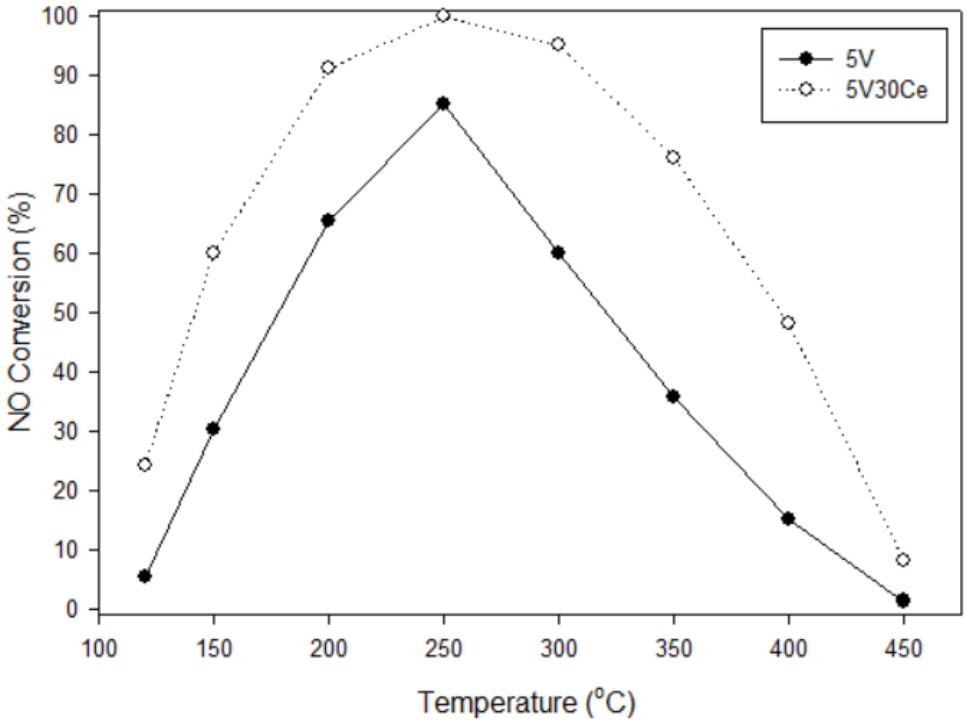

Figure 4.10 The NO conversion of V_2O_5/TiO2 catalyst and V_2O_5-CeO_2/TiO2 catalyst.

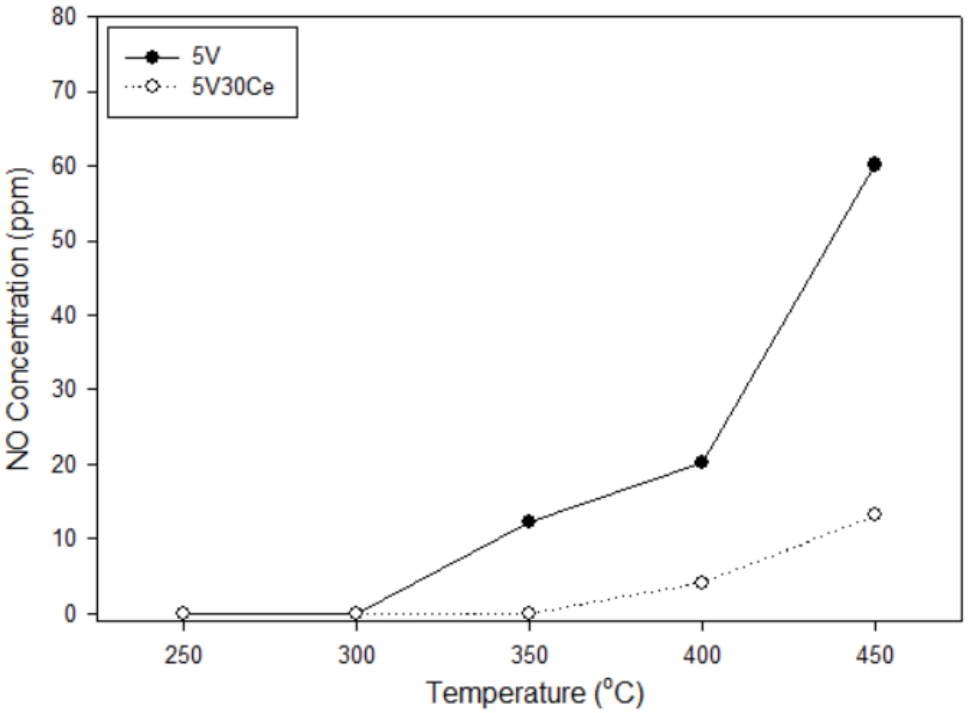

Figure 4.11 NO Concentration of V_2O_5/TiO_2 catalyst and V_2O_5-CeO_2/TiO_2 catalyst

Gibbs free energy, denoted G, combines enthalpy and entropy into a single value. The change in free energy, ΔG, is equal to the sum of the enthalpy plus the product of the temperature and entropy of the system. ΔG can predict the direction of the chemical reaction under constant temperature conditions. In this case, we have compared gibbs free energy of SCR reaction and ammonia oxidation reaction at 250 °C and 450°C to explain selectivity of the reaction at following temperature.

$$4NO + 4NH_3 + O_2 \longrightarrow 4N_2 + 6H_2O \qquad (1.1)$$

$$4NH_3 + 5O_2 \longrightarrow 4NO + 6H_2O \qquad (1.3)$$

The gibbs free energy of SCR reaction (Equation 1.1) at 250 and 450°C is -1016.84 and -836.32 kJ/mol. From this result shown that the SCR reaction appeared to happen at temperature 250 °C greater than 450°C. In case ammonia oxidation reaction (Equation 1.2) the gibbs free energy at 250 and 450°C is -978.18 and -1353.59 kJ/mol, the result shown that the ammonia oxidation reaction appeared to happen

at temperature 450 ^{o}C greater than 250^{o}C. The ammonia oxidation reaction occur when the reaction temperature increases to high temperature.

4.4 Effect of water vapor and sulfur dioxide on the catalysts.

Water vapor and sulfur dioxide are the main components in flue gas, so it is very important for industrial application to investigate the effect of water vapor and sulfur dioxide on SCR activities of catalysts. In this section the activity of V_2O_5-TiO_2 and CeO_2-V_2O_5-TiO_2 catalysts were investigated in the presence of water vapor and sulfur dioxide. Water vapor and sulfur dioxide were added into feed gas. The composition of feed gas mixture contained 120ppm NO, 120ppm NH_3, 30 ppm SO_2. The concentration of O_2 and water vapor were 15% by volume. And the rest was balanced with N_2.

4.4.1 Effect of sulfur dioxide on the activity of V_2O_5/TiO_2 and CeO_2-V_2O_5/TiO_2 catalysts.

In this study, sulfur dioxide is fed into the system to determine this effect. The composition of feed gas mixture contained 120ppm NO, 120ppm NH_3, 30 ppm SO_2. The concentration of O_2 was 15% by volume. And the rest was balanced with N_2.

The experimental result in Figures 4.12 and 4.13 is shown that when sulfur dioxide is added into the system, the activities of catalyst at low temperature are increases and higher than no present sulfur dioxide. But at high temperature the activity of catalyst are decreases because the ammonia oxidation.

According to Zhanggen Huang (2004), the V_2O_5/AC catalyst activity increase when the sulfur dioxide was added in to the system. The results are attributed to the formation of sulfate species on the catalyst surface, which results in increased catalyst surface acidity and NH_3 adsorption.

The activity of catalysts at high temperature is lower than without sulfur dioxide because the ammonia oxidation appeared to happen at high temperature. The experimental results as shown in Figures 4.14 and 4.15.

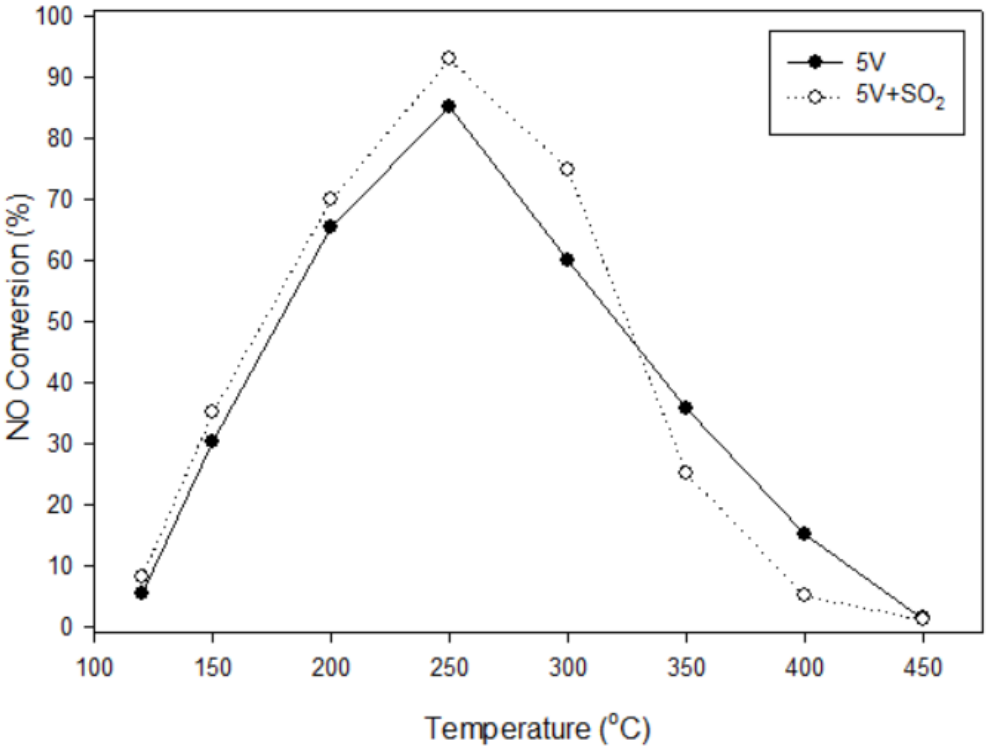

Figure 4.12 Effect of sulfur dioxide on NO conversion of V_2O_5/TiO_2 Catalyst

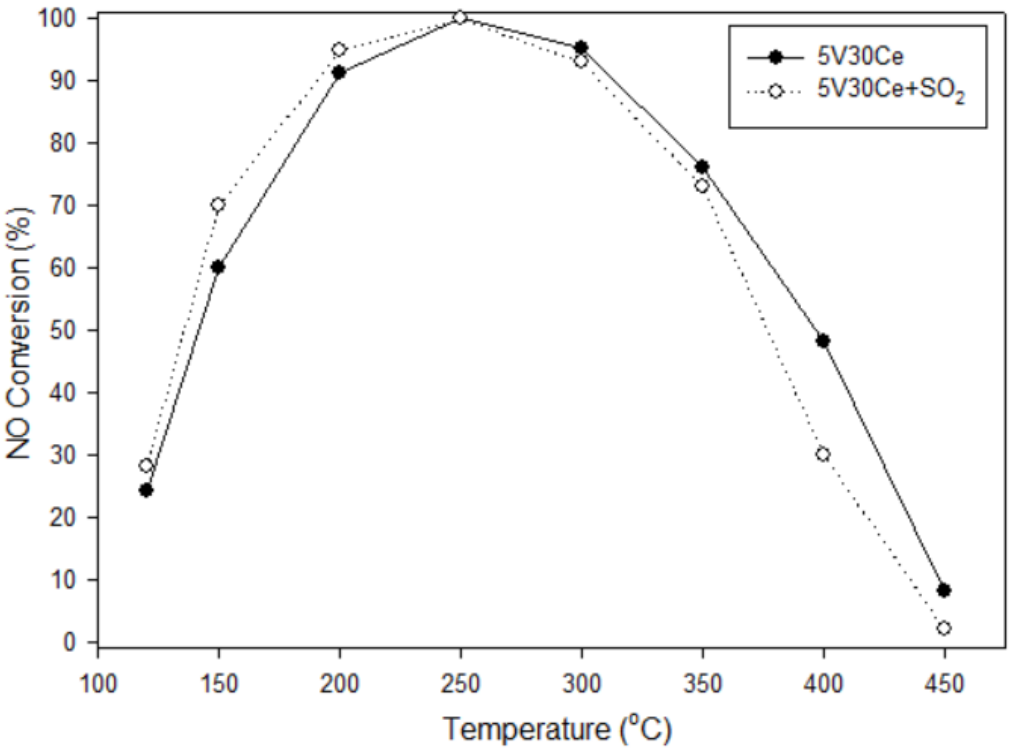

Figure 4.13 Effect of sulfur dioxide on NO conversion of CeO_2-V_2O_5/TiO_2 Catalyst

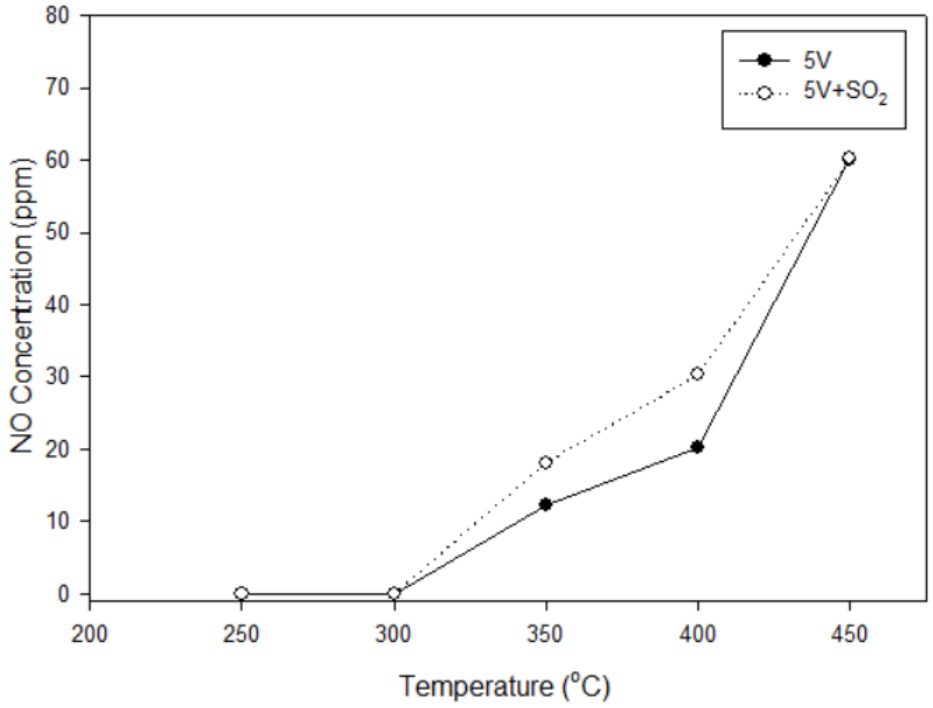

Figure 4.14 Effect of sulfur dioxide on ammonia oxidation reaction of V_2O_5-TiO_2 Catalyst

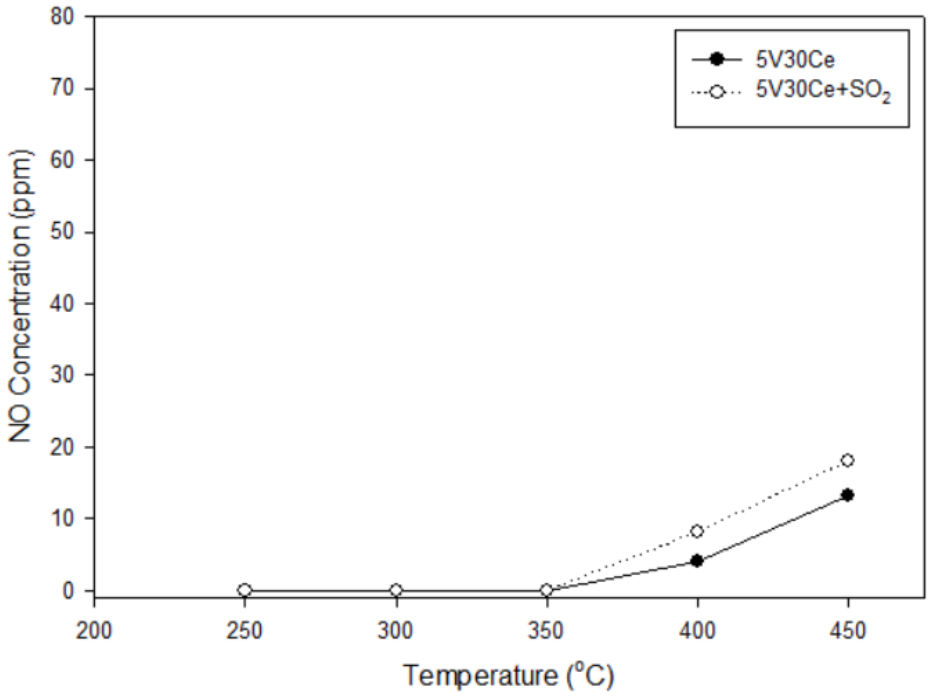

Figure 4.15 Effect of sulfur dioxide on ammonia oxidation reaction of CeO_2-V_2O_5/TiO_2 Catalyst

4.4.2 Effect of water vapor on the activity of V_2O_5/TiO_2 and CeO_2-V_2O_5/TiO_2 catalysts.

In this study, water vapor is fed into the system to determine this effect. The composition of feed gas mixture contained 120ppm NO, 120ppm NH_3. The concentration of O_2 and water vapor were 15% by volume. And the rest was balanced with N_2.

The experimental result in Figures 4.16 and 4.17 is shown that when water vapor is added into the system, the activities of catalyst at low temperature are decreased and lower than no present of water vapor. Although it is not clear in mechanism at present, it is likely that the decrease in NO conversion in this period is caused by increased adsorption of water vapor on active sites of the catalyst compete with ammonia by capillary condensation of water vapor in some of the pores of the catalyst. (Huang et al., 2002)

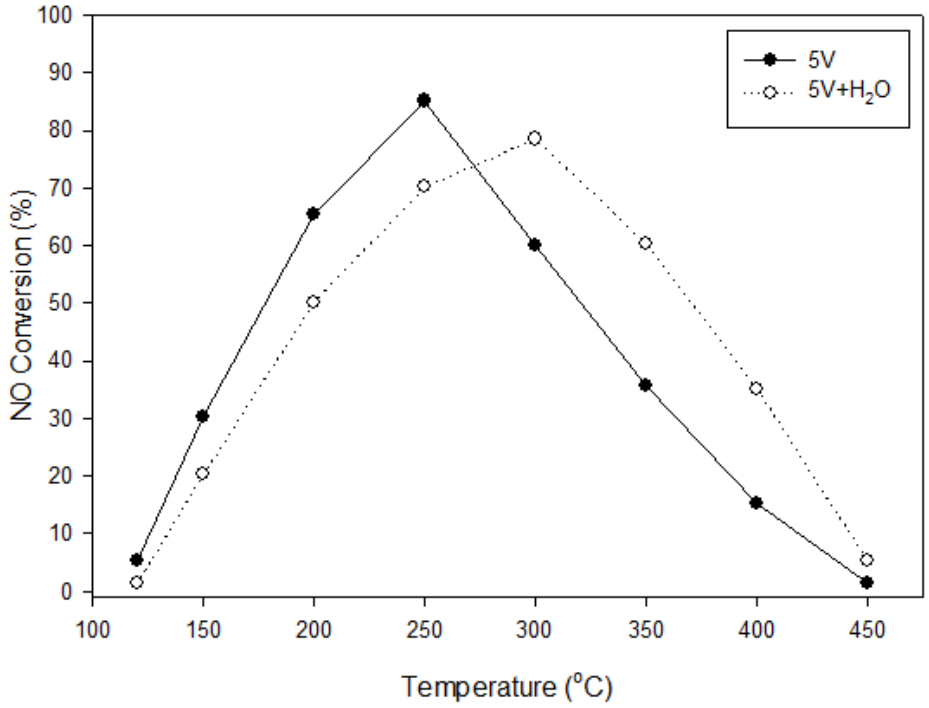

Figure 4.16 Effect of water vapor on NO conversion of V_2O_5/TiO_2 Catalyst

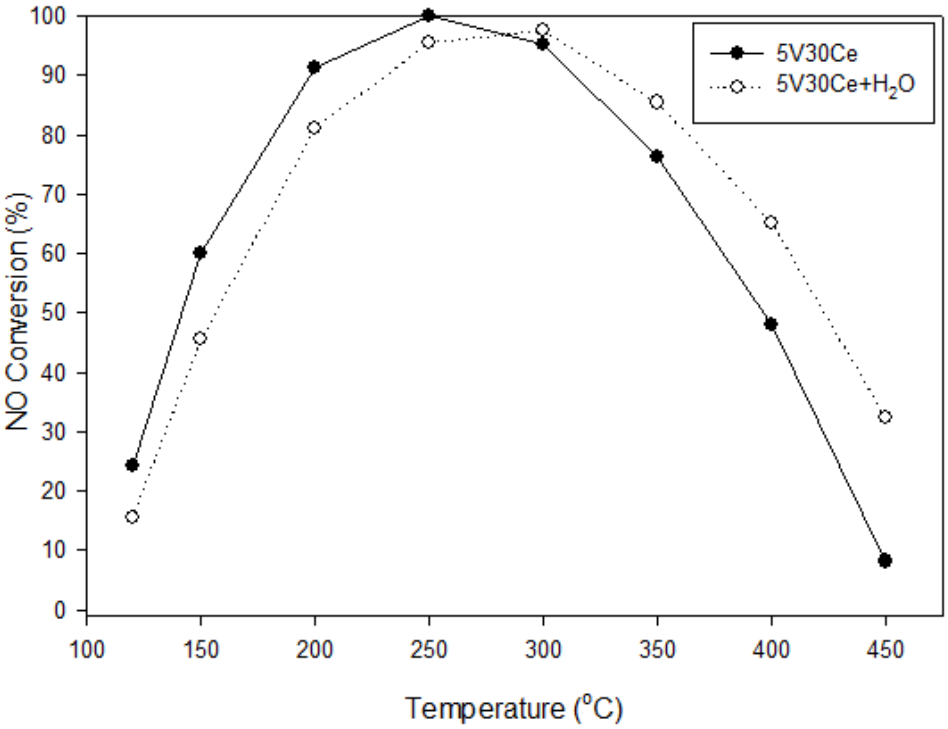

Figure 4.17 Effect of water vapor on NO conversion of CeO_2-V_2O_5/TiO_2 Catalyst

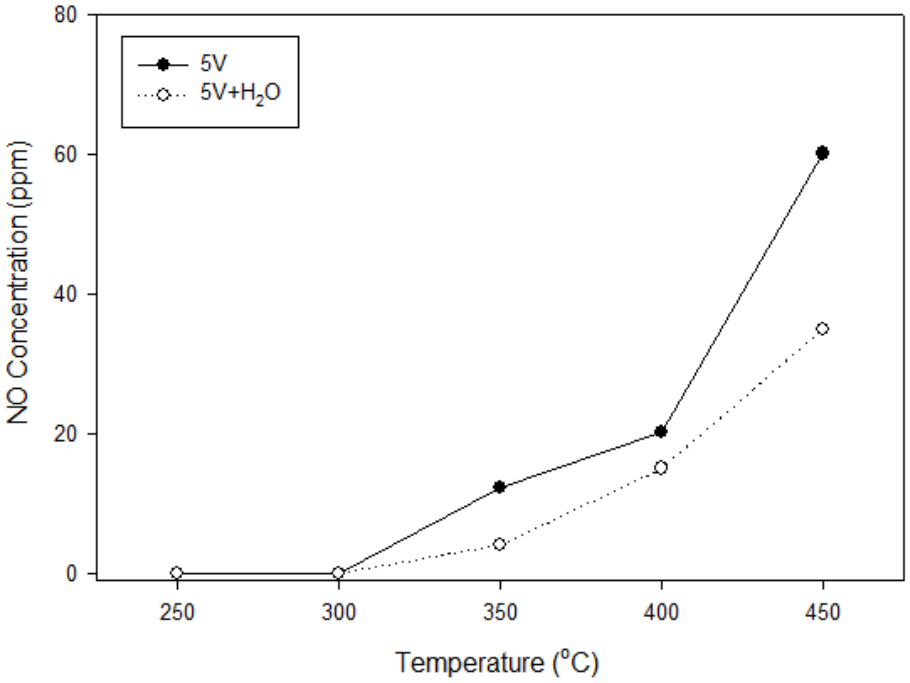

Figure 4.18 Effect of water vapor on Ammonia Oxidation reaction of V_2O_5/TiO_2 Catalyst

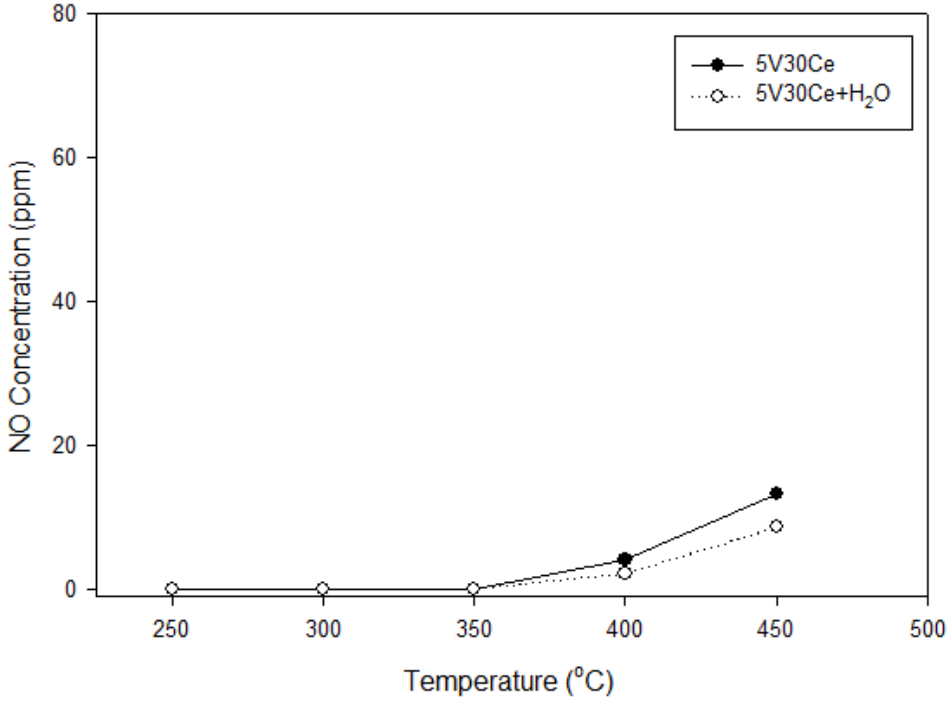

Figure 4.19 Effect of water vapor on ammonia oxidation reaction of CeO_2-V_2O_5/TiO_2 Catalyst

But at high temperature the activity of catalyst increased. Moreover, it is believed that water vapor could competitively adsorb with NH_3 on the site which oxidized NH_3 to NO. The blocking of this site resulted in lower NH_3 oxidation reaction. Water vapor in the feed gas were tend to improve the catalyst activity at high temperature. The experimental results as shown in Figures 4.18 and 4.19.

4.4.3 Effect of water vapor and sulfur dioxide on the activity of V_2O_5/TiO_2 and CeO_2-V_2O_5/TiO_2 catalysts.

In this study, water vapor and sulfur dioxide are fed into the system to determine this effect. The composition of feed gas mixture contained 120ppm NO, 120ppm NH_3. The concentration of O_2 and water vapor were 15% by volume. And the rest was balanced with N_2. The temperature was set constant at 250°C (The maximum activity in following study), to determine the effect of water vapor and sulfur dioxide on the activity of catalyst and study stability of catalyst. Moreover, the stability of catalyst was also investigated.

The experimental result in Figure 4.20 shows the influence of water vapor and sulfur dioxide on the activity of V_2O_5/TiO_2 catalyst. Before adding water vapor and sulfur dioxide the SCR reaction was stabilized for 5 hours at 250°C, NO conversion 89%. When sulfur dioxide was added, NO conversion increased to 91%. The result according to following study in the section 4.4.1. Accord. The results are attributed to the formation of sulfate species on the catalyst surface, which results in increased catalyst surface acidity and NH_3 adsorption (Zhanggen Huang et al., 2004). The catalyst activity remained steady for 10 hours. Introduction of water vapor, at time on stream of 6 hours, the NO conversion was decreased continuously, until the time on stream 48 hours where the activity of the catalyst completely vanished.

The specific surface area of 5%V_2O_5/TiO_2 catalysts before and after sulfur dioxide and water vapor were added to the system. The NO conversion was decreased until complete deactivation of the catalyst corresponds to the loss of

specific surface area, decrease from 58.99 to 19.25 BET/$m^2 \bullet g^{-1}$ after adding water vapor and sulfur dioxide the system.

According to Zhanggen Huang (2006), the relatively “slow” deactivation of the catalyst is resulted from the deposition of ammonium sulfate salts on the catalyst surface, which blocks the pores of the catalyst. The increased deactivation rate of the catalyst with increasing water vapor content suggests that water vapor promotes the deposition of ammonium sulfate salts. It is important to note that ammonium sulfate salts form on the catalyst surface in the presence of sulfur dioxide and water vapor. The amount of ammonium sulfate salts on the catalyst surface determines its effect on the SCR activity. The effect of water vapor on the deposition of ammonium sulfate salts may result from an increase in its formation rate and from a decrease in its reaction rate with NO.

Although the actual mechanism for the catalyst deactivation is unknown at the present time, it is likely that the immediate decrease in catalyst activity upon the introduction of water vapor is caused by adsorption of water vapor on the active sites of the catalyst, as reported in the literature (Ronald,. 2001), as well as by loss of surface area resulted from capillary water vapor condensation in some of pore of catalyst.

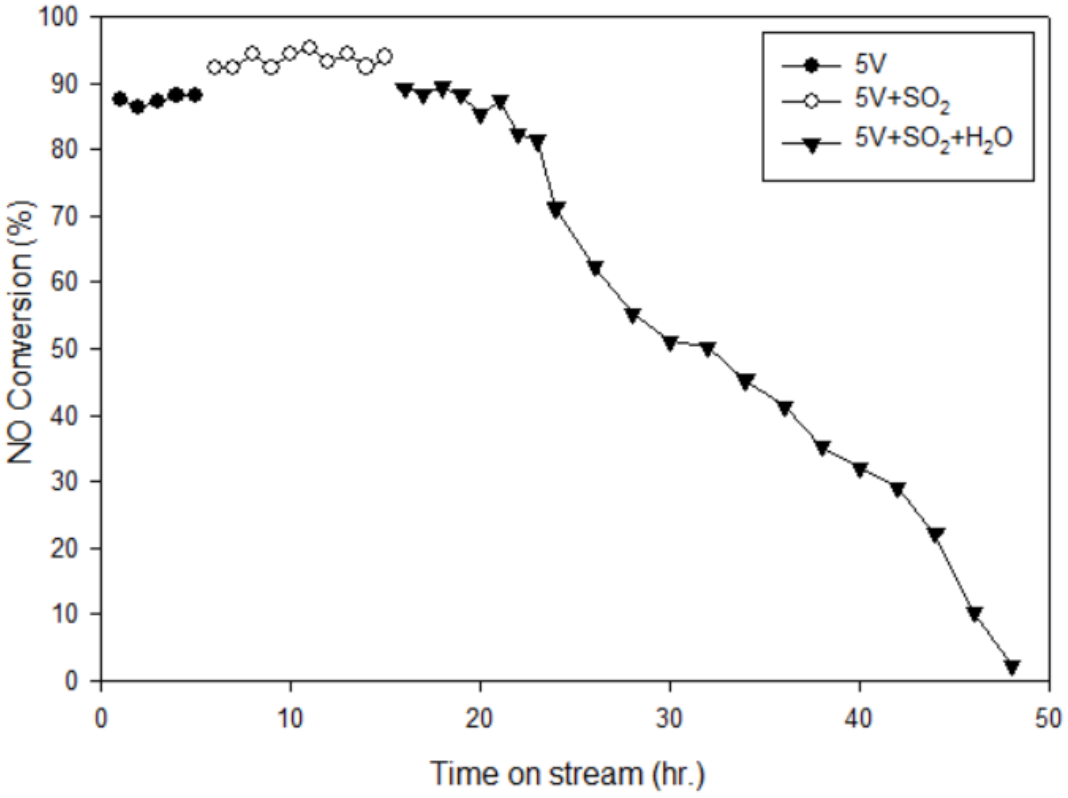

Figure 4.20 Temporal profile of NO conversion over V_2O_5/TiO_2 catalyst under the presence of sulfur dioxide and water vapor

Figure 4.21 shows the effect of water vapor and sulfur dioxide on the NO conversion of CeO_2-V_2O_5/TiO_2 catalyst. Before adding water vapor and sulfur dioxide the NO conversion was stabilized at 100% NO conversion for 5 hour at 250°C. When sulfur dioxide was added, NO conversion was also unchanged in 10 hour. In fact, the addition of sulfur dioxide, NO conversion will be increase. Because of the formation of sulfate species on the catalyst surface, this results in increased catalyst surface acidity and NH_3 adsorption. But NO conversion unchanged, because it is a maximum conversion. Introduction of water vapor at time on stream 6 hour. The NO conversion decreased slowly to about 89%, then NO conversion unchanged in 32 hour.

The results suggest that the addition of cerium oxide in the V_2O_5/TiO_2 catalyst, the catalysts showed an excellent resist to water vapor and sulfur dioxide under our test conditions.

According to XU et al. ,The catalyst that have Ce Content from 5% to higher value showed high activity in the temperature rang 274-400°C. All the catalyst can resist to sulfur dioxide and water vapor under test condition.

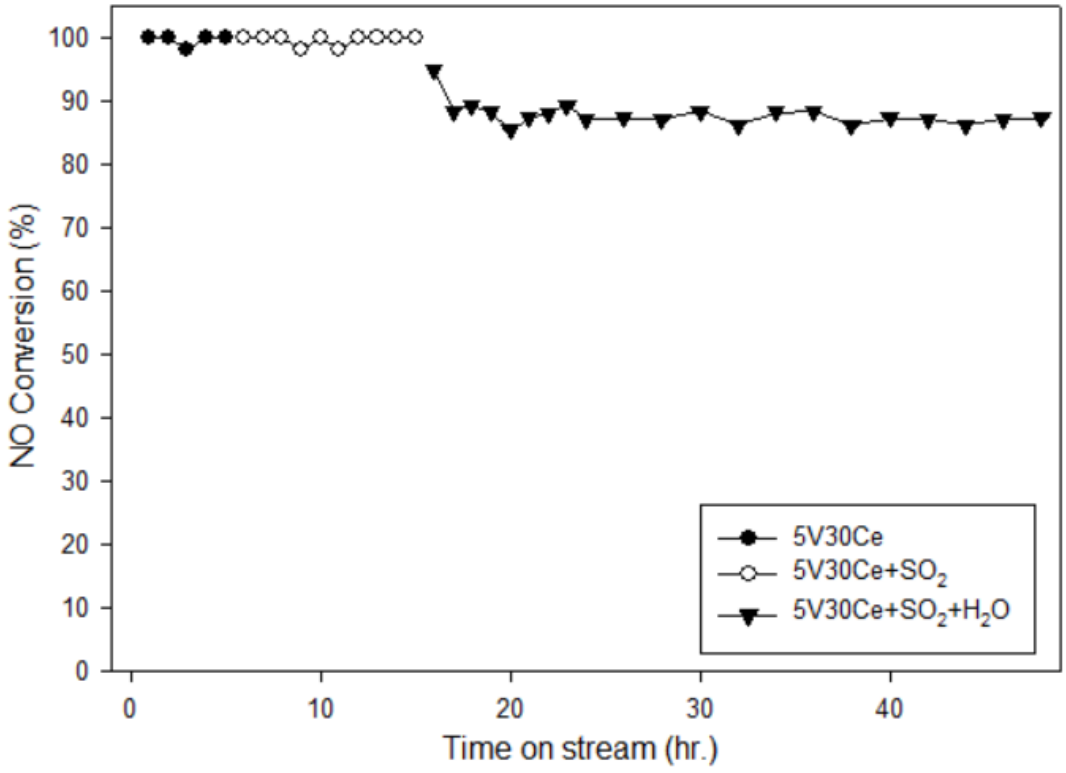

Figure 4.21 Temporal profile of NO conversion over CeO_2-V_2O_5/TiO_2 catalyst under the presence of sulfur dioxide and water vapor

CHAPTER V
CONCLUSIONS AND RECOMMENDATIONS

In this chapter, section 5.1 provides the conclusions obtained from the experiment results. Additionally, recommendations for further study are also given in the end of this chapter.

5.1 Conclusions

The catalyst containing 5 %wt. V_2O_5, 30 %wt. CeO_2 was achieve superior activity at low temperature and exhibit the highest activity at 250°C. The addition of CeO_2 increased the catalyst surface area and the total acid site of catalyst, leading to high catalytic activity. The extent of ammonia oxidation increased with the reaction temperature and the vanadium content in catalysts. Addition of cerium to catalyst inhibited ammonia oxidation reaction and retained the SCR activity at high temperature. In the present of H_2O and SO_2, the addition of cerium oxide in the V_2O_5-TiO_2 catalyst, the catalysts showed an excellent resist to water vapor and sulfur dioxide under our test conditions.

5.2 Recommendations

1. Formation of nitrous oxide (N_2O) from the ammonia oxidation reaction and SCR reaction was also investigated

2. Investigated the actual mechanism for the catalyst deactivation by sulfur dioxide and water vapor

3. Investigation of dispersion of metal on the catalyst.

4. Study the catalyst was coated on a monolith.

REFERENCES

Busca G., Liettib L., Ramisa G. and Bertic F. Chemical and mechanistic aspects of the selective catalytic reduction of NO_x by ammonia over oxide catalysts: A review. Applied Catalysis B: Environmental 18 (1998): 1-36.

Boudali L. K., Ghorbel A. and Grange P. Characterization and reactivity of WO_3-V_2O_5 supported on sulfated titanium pillared clay catalysts for the SCR-NO reaction. C. R. Chimie 12 (2009): 1-8.

Beretta A., Orsenigo G., Ferlazzo N., Tronconi E. and Forzatti P. Analysis of theperformance of plate-type monolithic catalysts for selective catalytic reduction deNOx applications. Ind. Eng. Chem. Res. 37 (1998): 2623-2633.

Gao, X., Jiang, Y., Zhong, Y., Luo, Z., and Cen, K. The activity and characterization of CeO_2-TiO_2 catalysts prepared by the sol-gel method for selective catalytic reduction of NO with NH3. Journal of Hazardous Materials 174 (2010): 734-739.

Gomez-Gracial, M.A., Pitchon, V., and Kiennemann, A. Pollution by nitrogen oxides: an approach to NO_x abatement by using sorbing catalytic materials. Environment International 31 (2005): 445-467.

Goo, J.H., Irfan, M.F., Kim, S.D., and Hong, S.C. Effects of NO_2 and SO_2 on selective catalytic reduction of nitrogen oxides by ammonia. Chemosphere 67 (2007): 718-723.

Huang Z., Zhu Z. and Liu Z. Combined effect of H_2O and SO_2 on V_2O_5/AC catalysts for NO reduction with ammonia at lower temperatures. Applied Catalysis B: Environmental 39 (2002): 361–368.

Juan, A.M., Malcolm, Y., Pedro, A., Silvia, S., and Jesus, B. Nitrous oxide formation in low temperature selective catalytic reduction of nitrogen oxides with V_2O_5/TiO_2 catalysts. Applied catalysis 70 (2007): 330-334.Ronald, M., Heck, 1999, Catalysis Today, 53, 519–523.

Jung S. M. and Grange P., DRIFTS investigation of V=O behavior and its relations with the reactivity of ammonia oxidation and selective catalytic reduction of NO over V_2O_5 catalyst. Applied Catalysis B: Environmental 36 (2002): 325–332.

Roy, S., Hegde, M.S., and Madras, G,.Catalysis for Nox adatement Appiled Energy 86 (2009): 2283-2297.

Tang X., Hao J., Xu W. and Li J. Low temperature selective catalytic reduction of NO_X with NH_3 over amorphous MnO_X catalysts prepared by three methods. Catalyst Communication 8 (2007): 329-334.

Tong, Z. Q., 2001, Industrial waste gas removal and utilization. Beijing: Chemical Industrial Press, 546.

Xu, W., Yu, Y., Zhang, C., and He, H. Selective catalytic reduction of NO by NH_3 over a Ce/TiO_2 catalyst. Catalysis communications 9 (2008): 1453-1457.

Zhu, H., She ,M., Kong, Y., Hong, J., Hu, Y., Liu, T., Dong, L., Chen, Y., Jian, C., Liu, Z. Characterization of copper oxide supported on ceria-modified anatase. Mol Catal A 219 (2004): 155–164.

APPENDICES

APPENDIX A

CALCULATION FOR CATALYST PREPARATION

Preparation of catalyst powder was shown as follows:

Reagent:

- Titanium (IV) isopropoxide (TTIP), $TiC_{12}H_{28}O_4$ (>99%; Aldrich Chemical)
- Ammonium metavanadate, NH_4VO_3 (>99.99%; Aldrich Chemical)
- Cerium (III) nitrate hexahydrate, $Ce(NO_3)_3 \cdot 6H_2O$ (>99.99%; Aldrich Chemical)
- Oxalic acid hydrate (Fluka)

A1. Calculation for the preparation of V_2O_5/TiO_2 catalyst powder

Example calculation for the preparation of 5%wt. V_2O_5 (5V catalyst)

Based on 2 g of catalyst support (TiO_2) used, the composition of the catalyst will be as follows:

TiO_2 (95% wt) = 2 g

V_2O_5 (5% wt) = $\frac{2 \times 0.05}{0.95}$ = 0.105 g

V_2O_5 0.105 g was prepared from NH_4VO_3, molecular weight of V_2O_5 is 181.879 g/mol and NH_4VO_3 is 116.98 g/mol

NH_4VO_3 required = $\frac{V_2O_5\ required}{MW\ of V_2O_5} \times$ MW of NH_4VO_3

= $2 \times \frac{0.105g}{181.87 \frac{g}{mol}} \times 116.98 \frac{g}{mol}$

= 0.01354 g

A2. Calculation for the preparation of CeO_2-V_2O_5/TiO_2 catalyst powder

Example calculation for the preparation of 5%wt. V_2O_5 and 10%wt.CeO_2 (5V10Ce catalyst)

Based on 2 g of catalyst support (TiO_2) used, the composition of the catalyst will be as follows:

TiO_2 (85% wt.) = 2 g

V_2O_5 (5% wt.) = $\frac{2\times0.05}{0.85}$ = 0.117g

CeO_2 (10% wt.) = $\frac{2\times0.1}{0.85}$ = 0.235 g

V_2O_5 0.117 g was prepared from NH_4VO_3, molecular weight of V_2O_5 is 181.879 g/mol and NH_4VO_3 is 116.98 g/mol

NH_4VO_3 required = $\frac{V_2O_5\ required}{MW\ of V_2O_5} \times$ MW of NH_4VO_3

= $2 \times \frac{0.117g}{181.87\ \frac{g}{mol}} \times 116.98\ \frac{g}{mol}$

= 0.151 g

CeO_2 0.235 g was prepared from $Ce(NO_3)_3 \cdot 6H_2O$, molecular weight of CeO_2 is 172.118 and $Ce(NO_3)_3 \cdot 6H_2O$ is 434.22 g/mol

$Ce(NO_3)_3 \cdot 6H_2O$ require = $\frac{CeO_2\ required}{MW\ of CeO_2} \times$ MW of $Ce(NO_3)_3 \cdot 6H_2O$

= $2 \times \frac{0.235g}{172.118\ \frac{g}{mol}} \times 434.23\ \frac{g}{mol}$

= 0.593 g

APPENDIX B

CALCULATION THE RESULT OF ICP-OES

The amounts of vanadium oxide (V_2O_5) and cerium oxide (CeO_2) in the catalyst were determined by inductively coupled plasma-optical emission spectroscopy (ICP-OES). The example of calculation is as following:

Example calculation for the metal content of 5%wt.V_2O_5 and 10%wt.CeO_2 (5V10Ce catalyst)

The amount of vanadium in the catalyst:

In the 3V10Ce catalyst 100 g, has 5%wt. V_2O_5 content.

Based on 0.011 g of 3V10Ce catalyst, has V_2O_5 content = 0.011 X 0.03

= 0.33 mg

The catalyst were digested by acid solution and diluted to 100 cm3

Therefore;

The catalyst concentration were $= \frac{0.33\ mg}{100\ cm^3} \text{ X } \frac{1000\ cm^3}{1\ L} = 3.3\ \frac{mg}{L}$ (ppm)

From the result of ICP-OES, the amount of vanadium (V) is 1.845 $\frac{mg}{L}$ (ppm)

∴ The concentration of $V_2O_5 = \frac{1.845 \times 181.879}{50.942 \times 2} = 3.293\ \frac{mg}{L}$ (ppm)

; M.W. of V_2O_5 =181.879 g/mol

M.W. of V =50.942 g/mol

Therefore;

Based on 0.011 g of 3V10Ce catalyst, has V_2O_5 content 3.3 ppm of V_2O_5

The V_2O_5 concentration of 3.293 ppm = $\frac{3.293 \times 3}{3.3}$ = 2.993 wt% of 3V10Ce catalyst

The amount of cerium in the catalyst:

In the 3V10Ce catalyst 100 g, has 10%wt. CeO_2 content.

Based on 0.011 g of 3V10Ce catalyst, has CeO_2 content = 0.011g X 0.1

= 1.1 mg

The catalyst were digested by acid solution and diluted to 100 cm3

Therefore;

The catalyst concentration were $= \frac{1.1\ mg}{100\ cm^3} \times \frac{1000\ cm^3}{1\ L} = 11\ \frac{mg}{L}$ (ppm) of CeO_2

From the result of ICP-OES, the amount of cerium (Ce) is 7.895 $\frac{mg}{L}$ (ppm)

∴ The concentration of $CeO_2 = \frac{7.895 \times 172.118}{140.12} = 9.698\ \frac{mg}{L}$ (ppm)

; M.W. of CeO_2 = 172.118 g/mol

M.W. of V = 140.12 g/mol

Therefore;

Based on 0.011 g of 3V10Ce catalyst, has CeO_2 content 11 ppm

The CeO_2 concentration of 3.293 ppm = $\frac{9.698 \times 10}{11}$ = 8.816 wt% of 3V10Ce catalyst

APPENDIX C

Data of result

C1. Data of V_2O_5/TiO2 catalyst on NO conversion

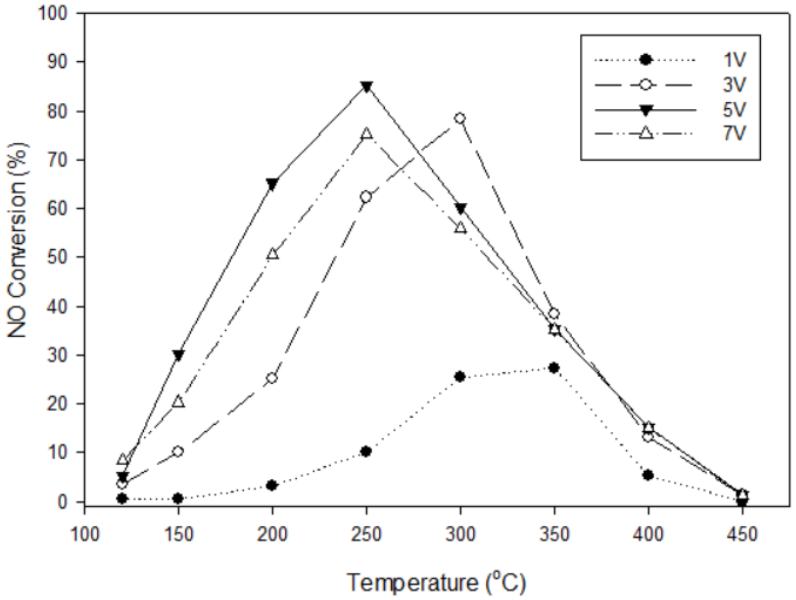

Figure 4.3 Effect of Vanadium loading on NO conversion

Table C1. Data of V_2O_5/TiO_2 catalyst

Temperature (°C)	NO Conversion (%)			
	1v	3v	5v	7v
120	0.00	3.56	5.32	8.36
150	0.00	10.03	30.22	20.41
200	3.13	25.25	65.23	50.37
250	10.13	62.29	85.25	75.26
300	25.35	78.37	60.26	55.98
350	27.35	38.25	35.24	35.26
400	5.35	13.21	15.24	15.12
450	0.00	1.24	1.27	1.31

C2. Data of CeO_2-V_2O_5/TiO_2 catalyst on NO conversion

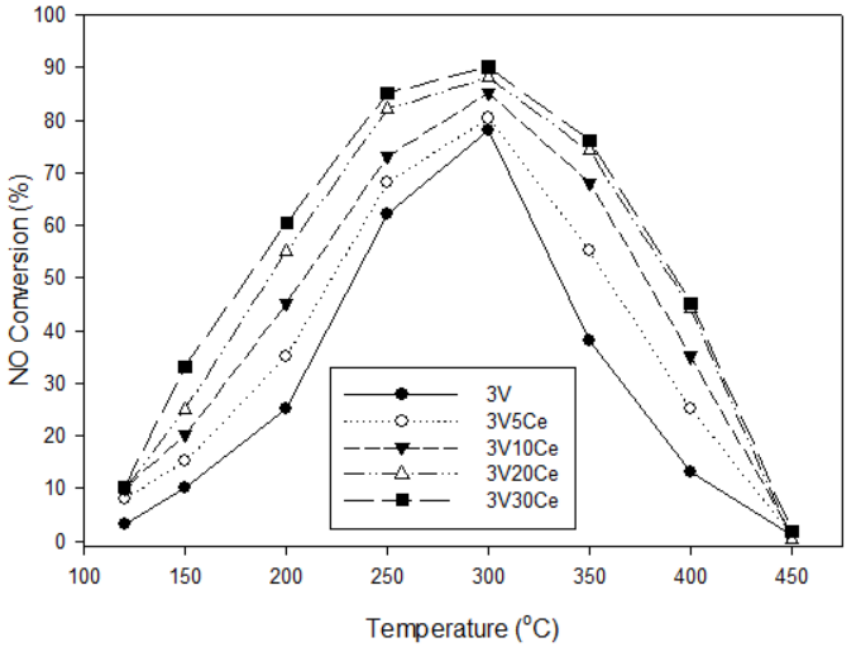

Figure 4.4 Effect of Cerium loading on 3%V_2O_5/TiO_2 catalysts.

Table C2. Data of CeO_2-3%V_2O_5/TiO_2 catalyst

Temperature (°C)	NO Conversion (%)				
	3v	3v5ce	3v10ce	3v20ce	3v30ce
120	3.25	8.01	10.01	10.00	10.21
150	10.03	15.95	20.45	25.02	33.13
200	25.22	35.13	45.13	55.14	60.37
250	62.85	68.55	73.36	82.33	85.87
300	78.96	80.32	85.63	88.53	90.63
350	38.42	55.12	68.20	74.12	76.21
400	13.13	25.13	35.13	44.21	45.25
450	1.36	1.05	1.27	0.23	1.91

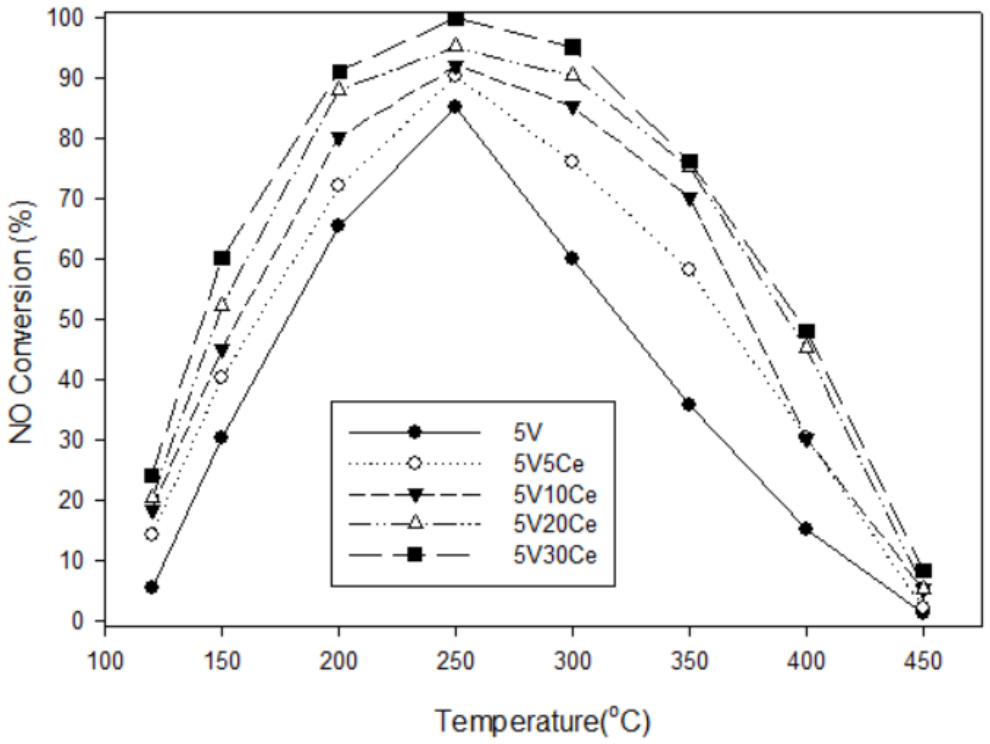

Figure 4.4 Effect of Cerium loading on $5V_2O_5/TiO_2$ catalysts.

Table C3. Data of CeO_2-5%V_2O_5/TiO_2 catalyst

Temperature (°C)	NO Conversion (%)				
	5v	5v5ce	5v10ce	5v20ce	5v30ce
120	5.25	14.54	18.21	20.33	24.12
150	30.13	40.37	45.13	52.25	60.13
200	65.37	72.13	80.37	88.12	91.21
250	85.18	90.37	92.13	95.25	100.00
300	60.25	76.96	85.43	90.37	95.24
350	35.63	58.13	70.35	75.24	76.36
400	15.13	30.37	30.74	45.12	48.54
450	1.27	1.99	5.12	5.25	8.95

C3. Data of ammonia oxidation reaction

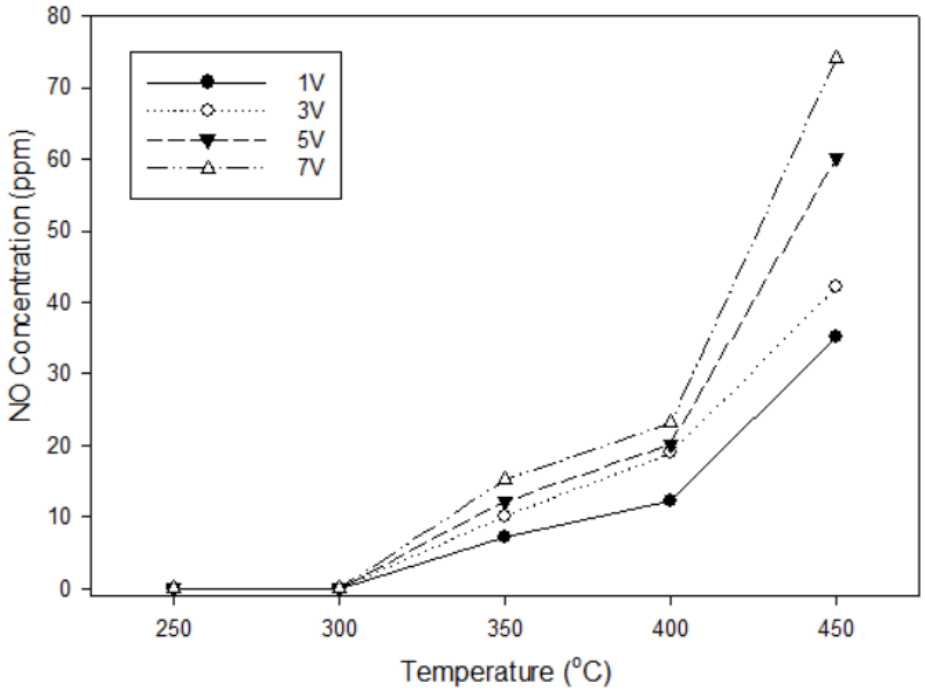

Figure 4.5 NO Concentration of V_2O_5/TiO_2 catalysts.

Table C4. NO Concentration of V_2O_5/TiO_2 catalysts.

Temperature (°C)	NO Concentration (ppm)			
	1v	3v	5v	7v
250	0	0	0	0
300	0	0	0	0
350	7.54	10.42	12.95	15.65
400	12.23	18.91	20.32	23.65
450	35.36	42.41	60.12	74.45

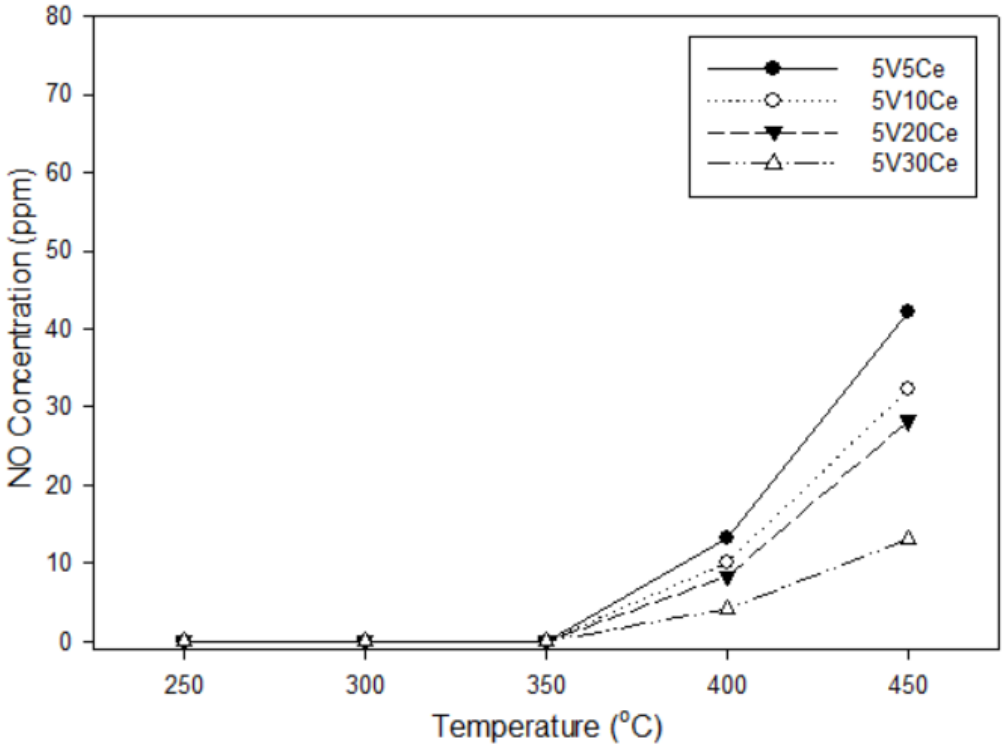

Figure 4.6 NO Concentration of V_2O_5-CeO_2/TiO_2 catalysts.

Table C5. NO Concentration of V_2O_5-CeO_2/TiO_2 catalysts.

Temperature (°C)	NO Concentration (ppm)			
	5v5ce	5v10ce	5v20ce	5v30ce
250	0.00	0.00	0.00	0.00
300	0.00	0.00	0.00	0.00
350	0.00	0.00	0.00	0.00
400	13.13	10.85	8.31	4.11
450	42.25	32.63	28.21	13.36

C4. Data of V_2O_5/TiO_2 catalyst on NO conversion at sulfur dioxide condition

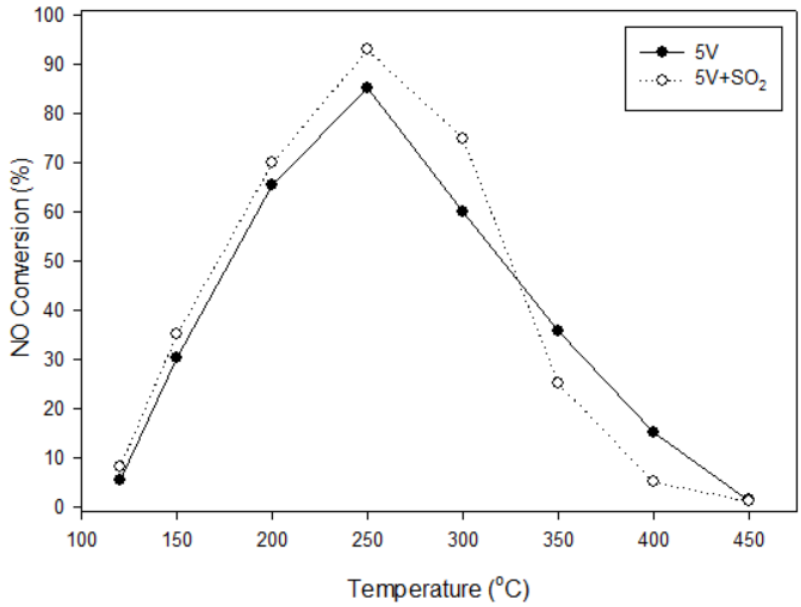

Figure4.7 Effect of sulfur dioxide on NO conversion of V_2O_5/TiO_2 Catalyst

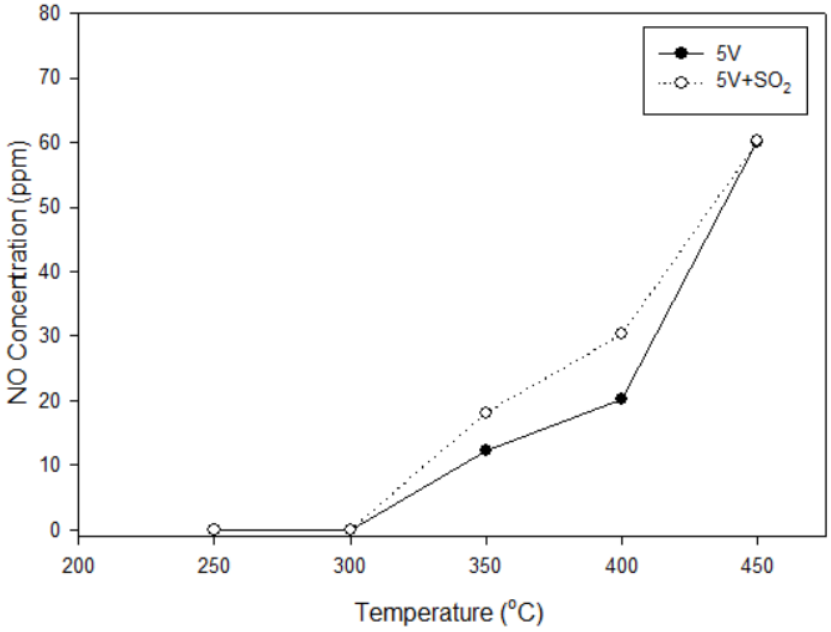

Figure4.9 Effect of sulfur dioxide on Ammonia Oxidation reaction of V_2O_5/TiO_2 Catalyst

Table C6. NO conversion of V_2O_5/TiO_2 Catalyst with/without sulfur dioxide in feed gas

Temperature (°C)	NO Conversion (%)	
	5v	5V+SO_2
120	5.32	8.58
150	30.22	35.62
200	65.23	70.12
250	85.25	93.85
300	60.26	75.98
350	35.24	25.12
400	15.24	5.56
450	1.27	1.98

Table C7. NO concentration (Ammonia oxidation reaction) of V_2O_5/TiO_2 Catalyst with/without sulfur dioxide in feed gas

Temperature (°C)	NO Concentration (ppm)	
	5v	5V+SO_2
250	0	0.00
300	0	0.00
350	12.95	18.13
400	20.32	30.29
450	60.12	60.25

C5. Data of CeO_2-V_2O_5/TiO_2 catalyst on NO conversion at sulfur dioxide condition

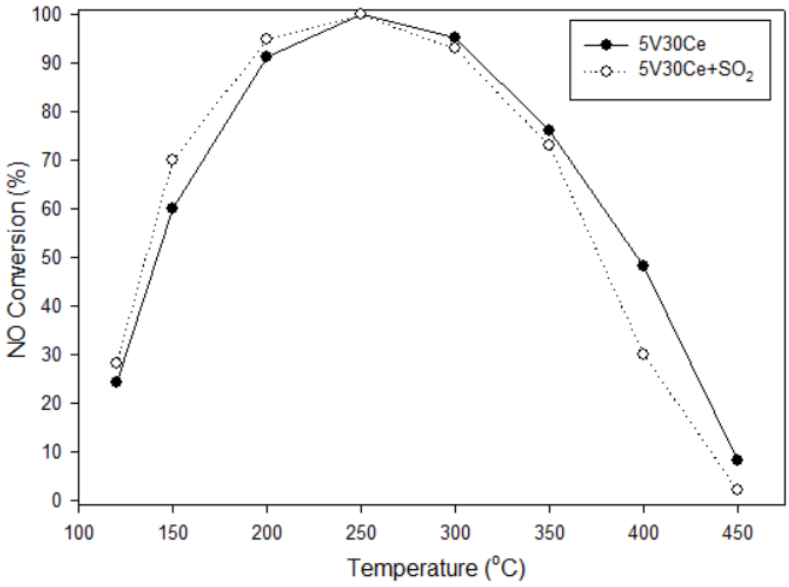

Figure4.8 Effect of sulfur dioxide on NO conversion of CeO_2-V_2O_5/TiO_2 Catalyst

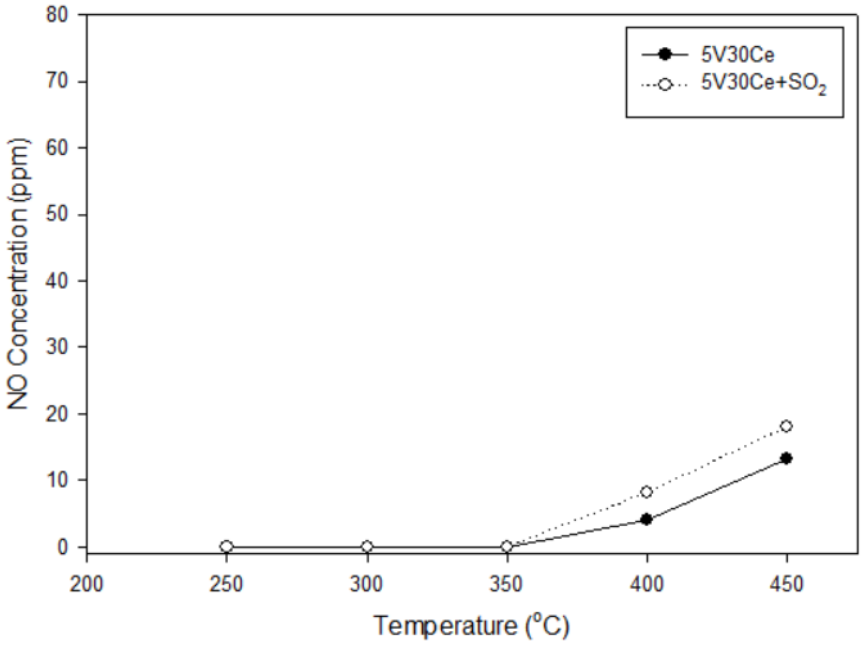

Figure4.10 Effect of sulfur dioxide on Ammonia Oxidation reaction of CeO_2-V_2O_5/TiO_2 Catalyst

Table C8. NO conversion of CeO_2-V_2O_5/TiO_2 Catalyst with/without sulfur dioxide in feed gas

Temperature (°C)	NO Conversion (%)	
	5V30Ce	5V30Ce+SO_2
120	24.12	28.25
150	60.13	70.32
200	91.21	95.15
250	100	100
300	95.24	93.69
350	76.36	73.23
400	48.54	30.75
450	8.95	2.36

Table C9. NO concentration (Ammonia oxidation reaction) of V_2O_5/TiO_2 Catalyst with/without sulfur dioxide in feed gas

Temperature (°C)	NO Concentration (ppm)	
	5V30Ce	5V30Ce+SO_2
250	0	0.00
300	0	0.00
350	0	0.00
400	4.11	8.22
450	13.36	18.12

C6. Data of V_2O_5/TiO_2 catalyst on NO conversion at water vapor condition

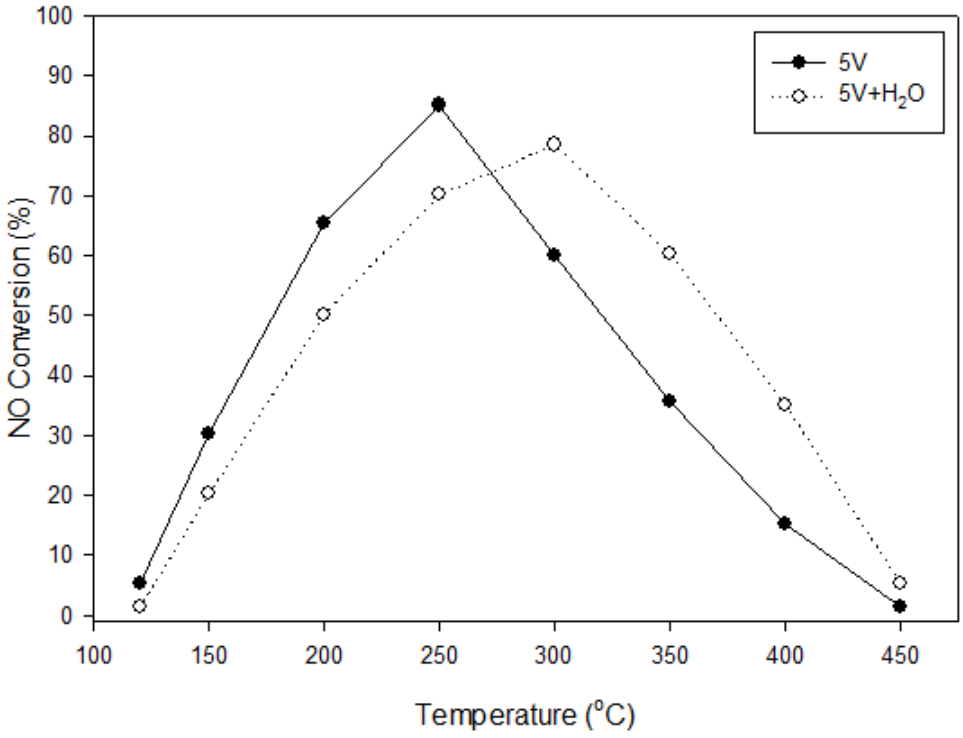

Figure4.15 Effect of water vapor on NO conversion of V_2O_5/TiO_2 Catalyst

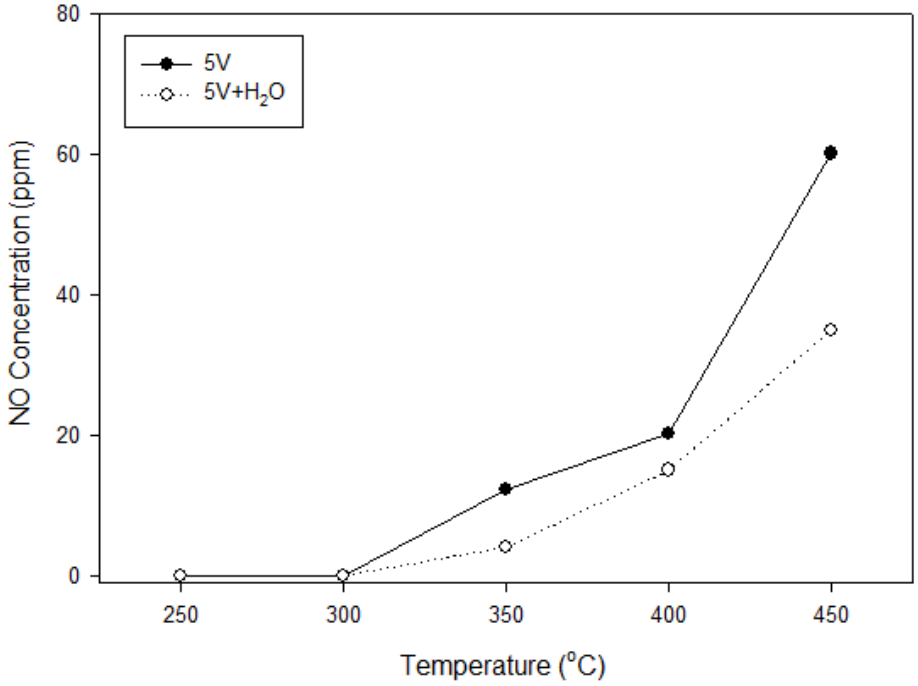

Figure4.17 Effect of water vapor on Ammonia Oxidation reaction of V_2O_5/TiO_2 Catalyst

Table C10. NO conversion of V_2O_5/TiO_2 Catalyst with/without water vapor in feed gas

Temperature (^{o}C)	NO Conversion (%)	
	5v	5V+H_2O
120	5.32	1.25
150	30.22	20.20
200	65.23	50.22
250	85.25	70.15
300	60.26	78.53
350	35.24	60.37
400	15.24	35.15
450	1.27	5.25

Table C11. NO concentration (Ammonia oxidation reaction) of V_2O_5/TiO_2 Catalyst with/without water vapor in feed gas

Temperature (^{o}C)	NO Concentration (ppm)	
	5v	5V+H_2O
250	0	0
300	0	0
350	12.95	4.85
400	20.32	15.45
450	60.12	35.63

C7. Data of CeO_2-V_2O_5/TiO_2 catalyst on NO conversion at water vapor condition

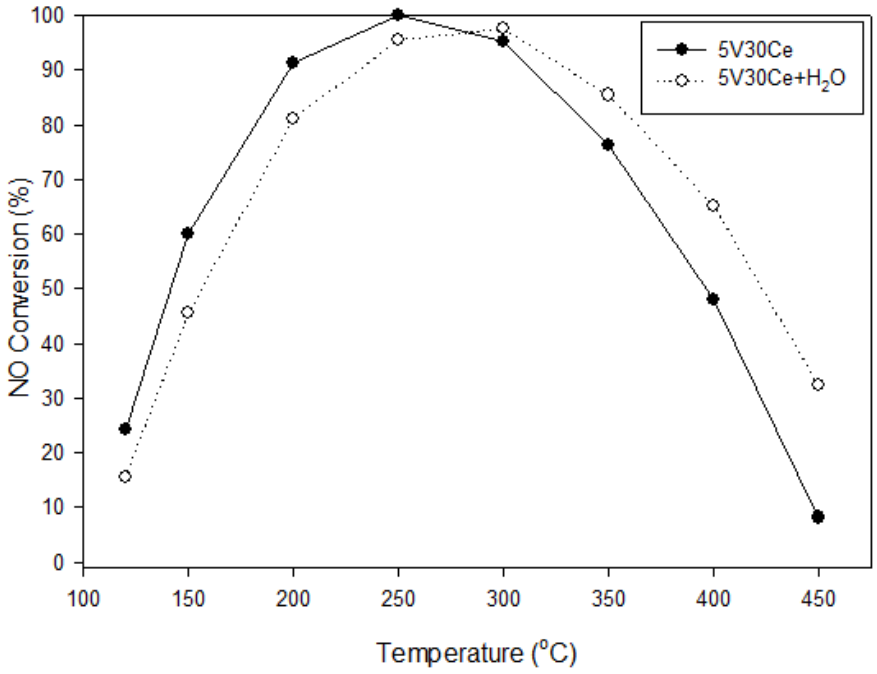

Figure4.16 Effect of water vapor on NO conversion of CeO_2-V_2O_5/TiO_2 Catalyst

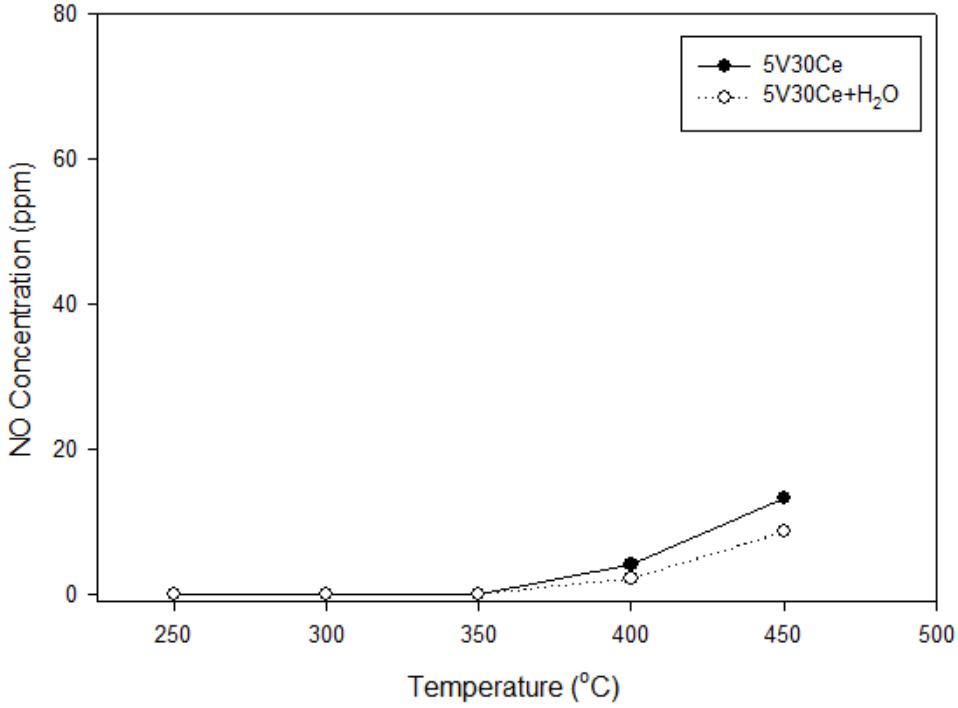

Figure4.18 Effect of water vapor on ammonia oxidation reaction of CeO_2-V_2O_5/TiO_2 Catalyst

Table C12. NO conversion of CeO_2-V_2O_5/TiO_2 Catalyst with/without water vapor in feed gas

Temperature (^{o}C)	NO Conversion (%)	
	5V30Ce	5V30Ce+H_2O
120	24.12	15.52
150	60.13	45.51
200	91.21	81.16
250	100	95.55
300	95.24	97.55
350	76.36	85.45
400	48.54	65.25
450	8.95	32.32

Table C13. NO concentration (Ammonia oxidation reaction) of V_2O_5/TiO2 Catalyst with/without water vapor in feed gas

Temperature (^{o}C)	NO Concentration (ppm)	
	5v30ce	5V30Ce+H_2O
120	24.12	15.52
150	60.13	45.51
200	91.21	81.16
250	100	95.55
300	95.24	97.55
350	76.36	85.45
400	48.54	65.25
450	8.95	32.32

C8. Data of V_2O_5/TiO_2 catalyst on NO conversion (Time on stream) at water vapor and sulfur dioxide condition

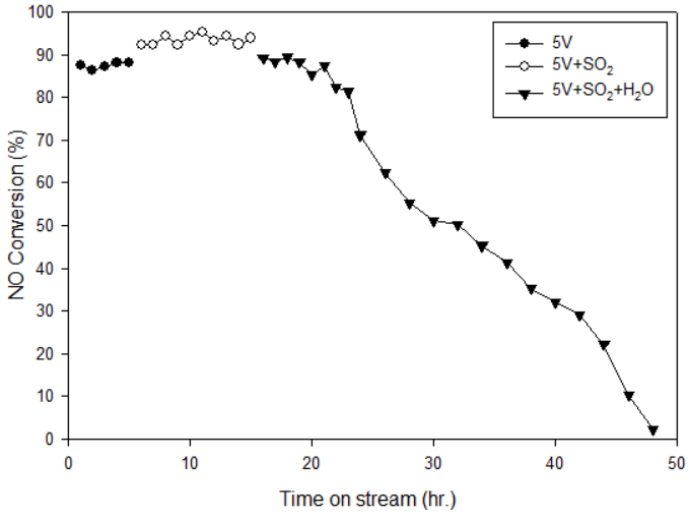

Figure 4.11 Temporal profile of NO conversion over V_2O_5/TiO_2 catalyst under the presence of sulfur dioxide and water vapor

Table C14. NO conversion (Time on stream) of V_2O_5/TiO_2 Catalyst

TOS (hr)	NO conversion (%)	TOS (hr)	NO conversion (%)	TOS (hr)	NO conversion (%)
1	87.45	13	94.29	26	62.37
2	86.21	14	92.42	28	55.75
3	87.32	15	93.91	30	51.23
4	88.02	16	89.99	32	50.21
5	88.21	17	88.30	34	45.32
6	92.25	18	89.39	36	41.23
7	92.17	19	88.76	38	35.23
8	94.23	20	85.43	40	32.12
9	92.55	21	87.34	42	29.12
10	94.34	22	82.35	44	22.12
11	95.34	23	81.34	46	10.85
12	93.12	24	71.23	48	2.35

C9. Data of CeO_2-V_2O_5/TiO_2 catalyst on NO conversion (Time on stream) at water vapor and sulfur dioxide condition

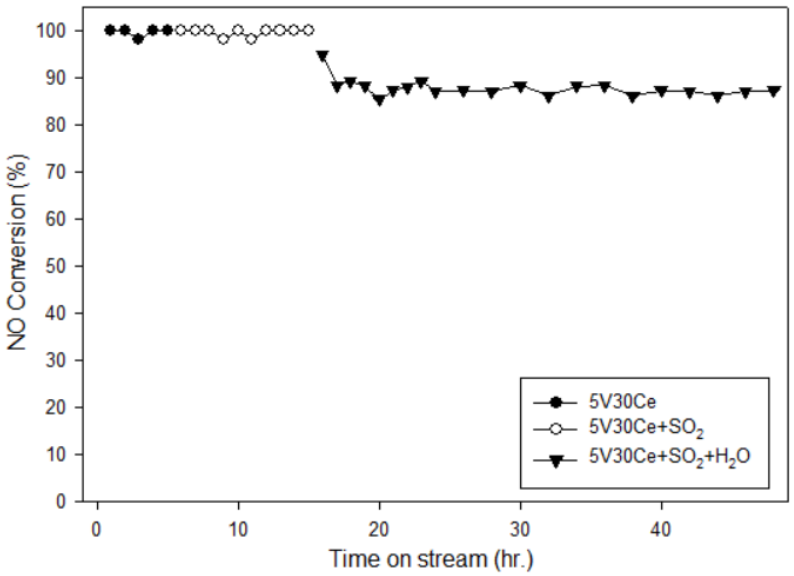

Figure 4.12 Temporal profile of NO conversion over CeO_2-V_2O_5/TiO_2 catalyst under the presence of sulfur dioxide and water vapor

Table C15. NO conversion (Time on stream) of CeO_2-V_2O_5/TiO_2 Catalyst

TOS (hr)	NO conversion (%)	TOS (hr)	NO conversion (%)	TOS (hr)	NO conversion (%)
1	100	13	100	26	87.33
2	100	14	100	28	87.23
3	98.58	15	100	30	88.34
4	100	16	95.57	32	86.23
5	100	17	88.30	34	88.23
6	100	18	89.39	36	88.31
7	100	19	88.23	38	86.24
8	100	20	85.43	40	87.32
9	98.75	21	87.34	42	87.23
10	100	22	88.12	44	86.23
11	98.65	23	89.30	46	87.23
12	100	24	87.23	48	87.34

APPENDIX D

CALIBRATING DATA FOR MASS FLOW METER

D1. Calibration data of mass flow meter are shown as follows:

Component of feed gas mixture as shown in Table 3.2

Table D1. feed gas for catalytic activity measurement

Feed gas	Supplier
NH_3 (10000 ppm in N_2)	BOC Scientific
SO_2 (10000 ppm in N_2)	BOC Scientific
NO (10000 ppm in N_2)	BOC Scientific
N_2 (99.999%)	Linde
O_2 (>=99.9%)	Linde

Used the bubble flow by passing the gas through the glass tube in oder to measure the time.

D1.1 Calibration data of ammonia

Used the bubble flow by passing the gas through the glass tube in order to measure the time. Record the time from scale 0 ml to 9 ml

Table D1. Calibration of ammonia

Mass flow controller (ml/min)	Time (min)			Time average (min)	Actual flow (ml/min)
	#1	#2	#3		
1	4.08	4.08	4.09	4.08	2.21
1.5	2.54	2.53	2.51	2.53	3.56
2	1.83	1.82	1.83	1.83	4.92
2.5	1.45	1.49	1.47	1.47	6.13
3	1.18	1.19	1.18	1.18	7.60

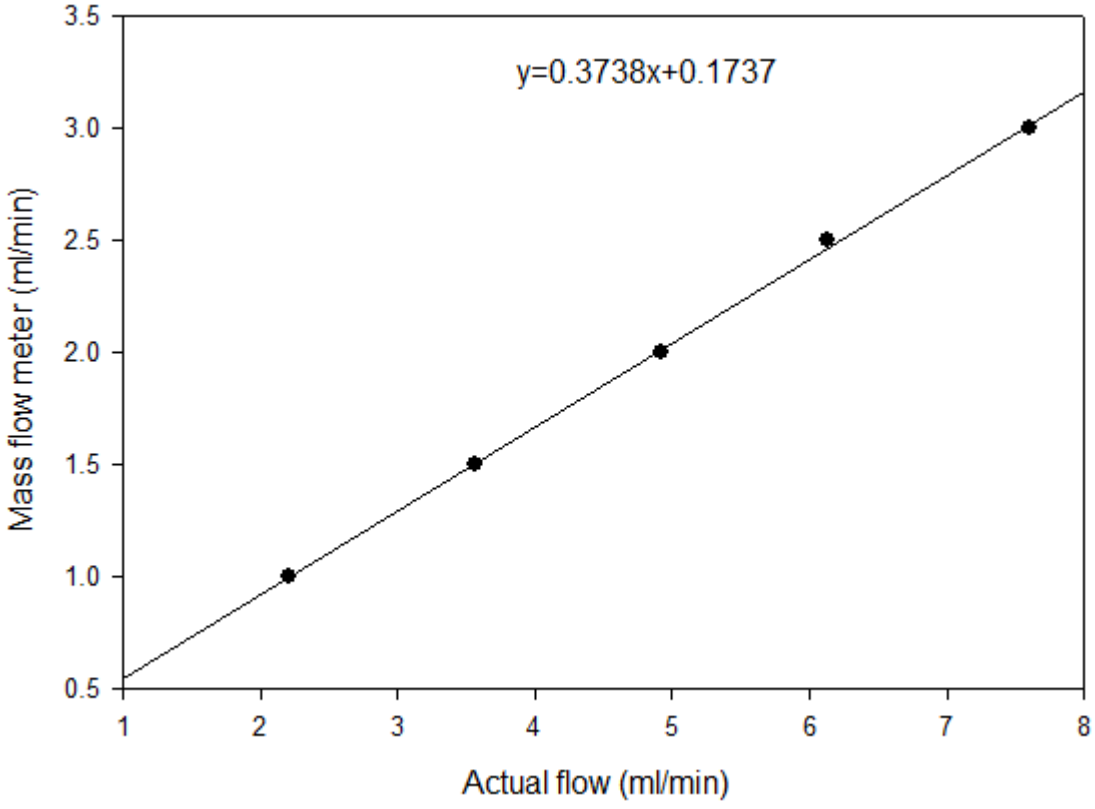

Figure D1. Calibration curve of ammonia

D1.2. Calibration data of nitrogen oxide

Used the bubble flow by passing the gas through the glass tube in order to measure the time. Record the time from scale 0 ml to 2 ml

Table D2. Calibration of nitrogen oxide

Mass flow controller (ml/min)	Time (min)			Time average (min)	Actual flow (ml/min)
	#1	#2	#3		
1	1.25	1.33	1.28	1.29	1.55
2	0.55	0.58	0.66	0.60	3.35
3	0.39	0.40	0.39	0.39	5.08
4	0.29	0.30	0.28	0.29	6.90
5	0.23	0.25	0.24	0.24	8.33

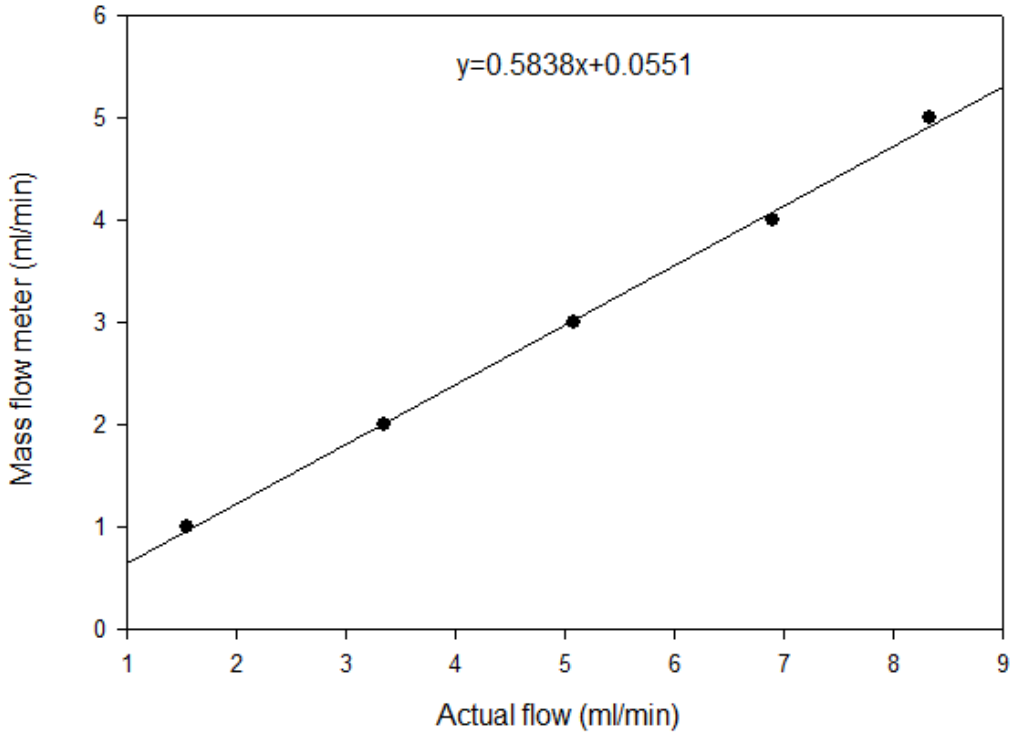

Figure D2. Calibration curve of nitrogen oxide

D1.3. Calibration data of oxygen

Used the bubble flow by passing the gas through the glass tube in order to measure the time. Record the time from scale 0 ml to 2 ml

Table D3. Calibration of oxygen

Mass flow controller (ml/min)	Time (min)			Time average (min)	Actual flow (ml/min)
	#1	#2	#3		
15	0.61	0.62	0.60	0.61	14.75
20	0.43	0.42	0.42	0.42	21.26
25	0.33	0.34	0.30	0.32	27.84
30	0.28	0.27	0.28	0.28	32.53
35	0.21	0.23	0.22	0.22	40.91
40	0.21	0.20	0.21	0.21	43.55

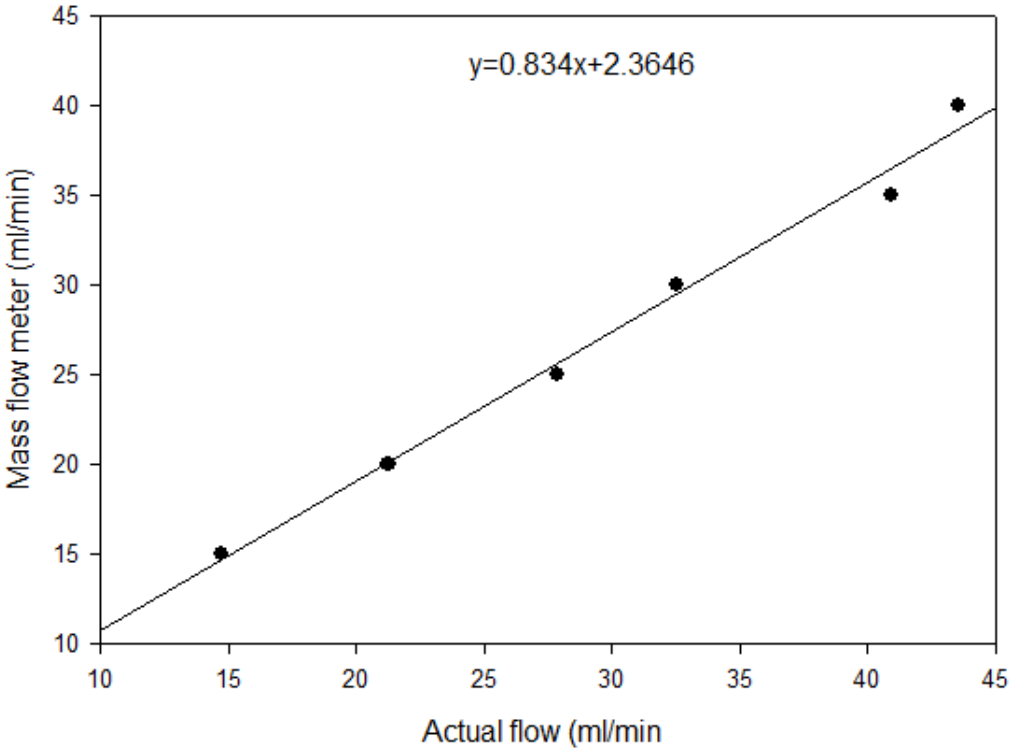

Figure D3. Calibration curve of oxygen

D1.4. Calibration data of sulfur dioxide

Used the bubble flow by passing the gas through the glass tube in order to measure the time.

Table D4. Calibration of sulfur dioxide

Mass flow controller (ml/min)	Volume bubble flow (ml)	Time (min)			Time average (min)	Actual flow (ml/min)
		#1	#2	#3		
0.4	1	2.01	2.00	1.99	2.00	0.50
0.6	2	2.35	2.37	2.37	2.36	0.85
0.8	3	2.38	2.37	2.36	2.37	1.27
1	9	5.51	5.52	5.50	5.51	1.63
1.5	9	3.48	3.49	3.50	3.49	2.58
2	9	2.51	2.57	2.52	2.53	3.55

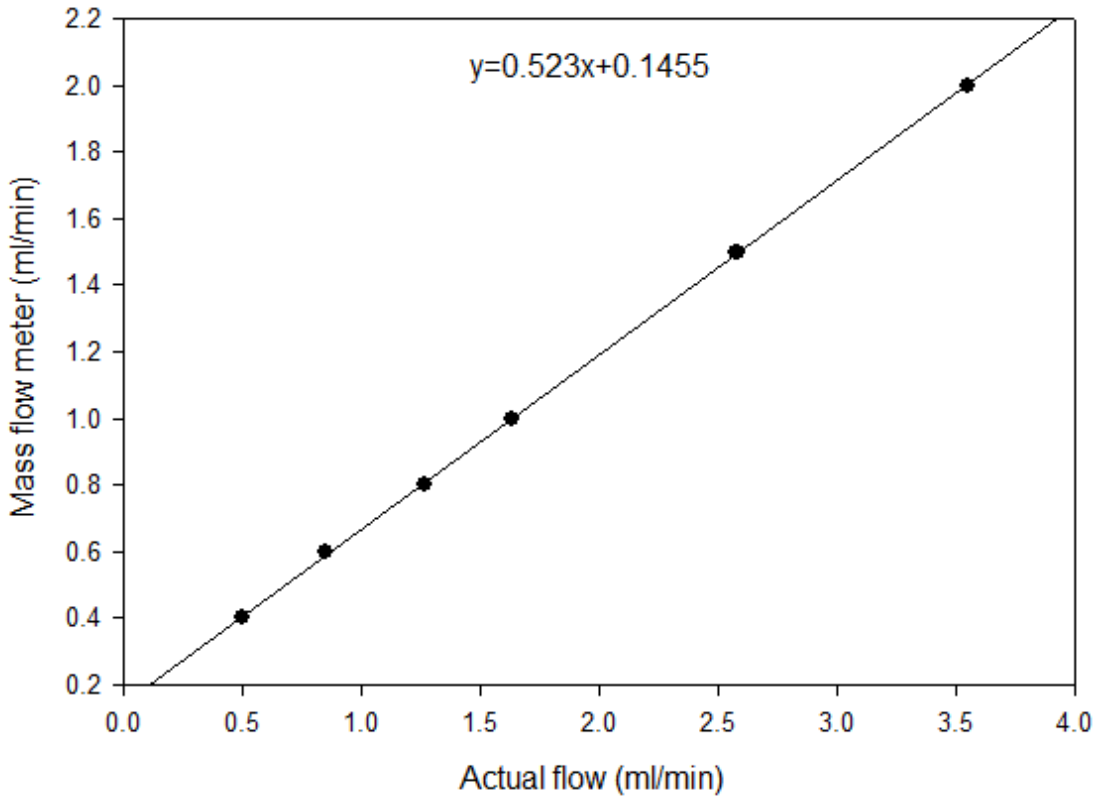

Figure D4. Calibration curve of sulfur dioxide

D1.5. Calibration data of nitrogen

Used the bubble flow by passing the gas through the glass tube in order to measure the time. Record the time from scale 0 ml to 2 ml

Table D5. Calibration of nitrogen

Mass flow controller (ml/min)	Time (min)			Time average (min)	Actual flow (ml/min)
	#1	#2	#3		
150	0.059	0.060	0.059	0.059	151.685
160	0.055	0.056	0.054	0.055	163.636
170	0.053	0.054	0.054	0.054	167.702
180	0.051	0.050	0.051	0.051	177.632
190	0.046	0.048	0.047	0.047	191.489
200	0.045	0.043	0.044	0.044	204.545

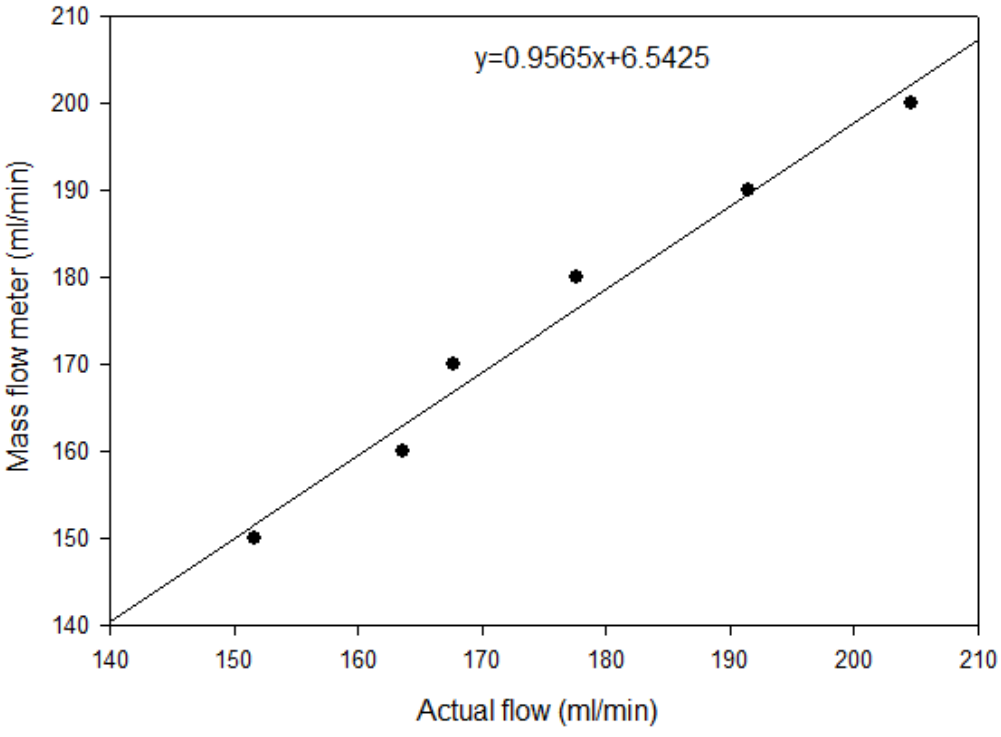

Figure D5. Calibration curve of nitrogen

APPENDIX E

DATA OF CALCULATION OF TOTAL ACID SITE

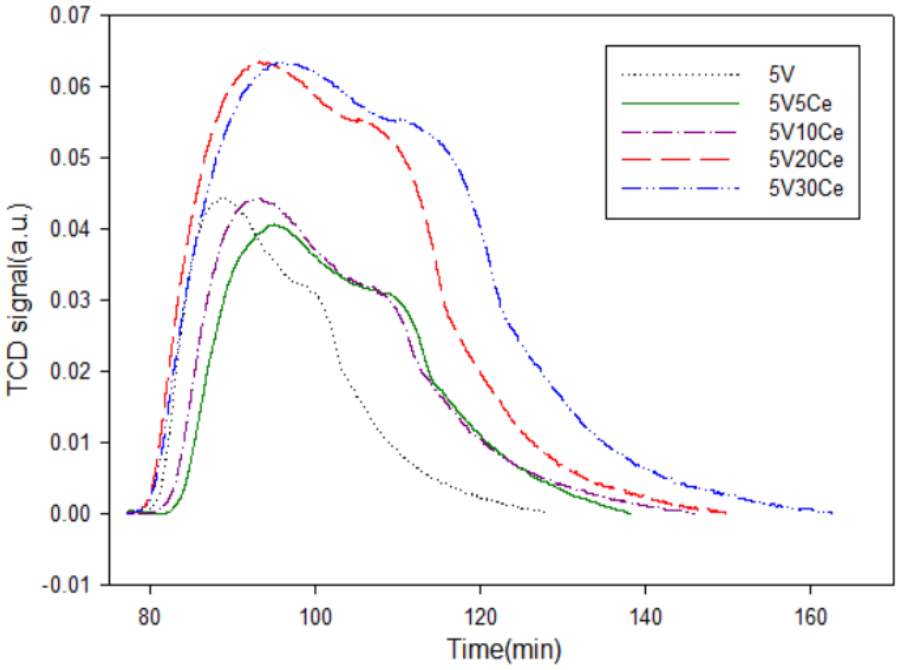

Figure 4.2 NH_3-TPD profiles of the catalyst.

Table E1. Data for calculation of total acid site

Catalyst	Area
5V	0.985
5V5Ce	1.058
5V10Ce	1.389
5V20Ce	1.875
5V30Ce	1.985

Calculation of total acid sites

For example, 5V30Ce catalyst, total acid site is calculated from the following step.

1. Calculation of total peak area to peak volume

From figure E1, the volume of NH_3 calculates from equation y = 16.885x

The volume of NH_3 = 16.885 x area

= 16.885 x 1.985

= 33.516 ml

2. Calculation for adsorbed volume of 15% NH_3

Adsorbed volume of 15% NH_3 = 0.15 x total peak volume

= 0.15 x 33.516

= 5.027 ml

3. The acid sites are calculated from the following equation

For 5V30Ce catalyst, 0.1001 g of this sample was measured, therefore

$$\text{The total acid site} = \frac{\textbf{Adsorbed volume(ml)} \times \textbf{101.325 Pa}}{8.314 \times 10^{-3}\frac{\textbf{Pa·ml}}{\textbf{K·µmol}} \times \textbf{298K} \times \textbf{weight of catalyst (g)}}$$

$$= \frac{5.027ml \times 101.325\ Pa}{8.314 \times 10^{-3}\frac{\textbf{Pa·ml}}{\textbf{K·µmol}} \times \textbf{298K} \times \textbf{0.1001g}}$$

= 2.054 mmol/g

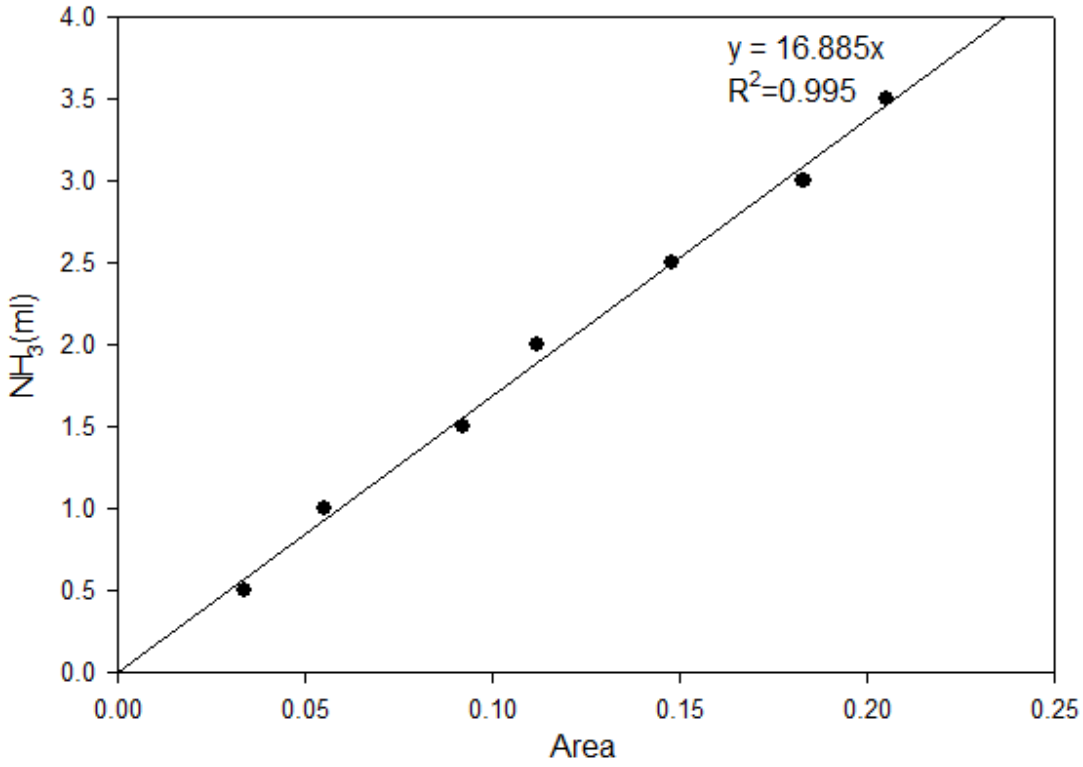

Figure E1. The calibration curve of ammonia

APPENDIX F

CALCULATION OF THE CRYSTALLITE SIZE

Calculation of the crystallite size by Debye-Scherrer equation

The crystallite size was calculate from the half-height width of the highest intensity diffraction peak of XRD patterns of titanium dioxide.

The crystallite size can be calculated from 2theta profile analysis, FWHM, by Debye-Scherrer equation that was suitable for particle size below 100 nm.

From Debye-Scherrer equation

$$D = \frac{K\lambda}{\beta\cos\theta} \qquad \text{(F.1)}$$

Where D = Crystallite size, Å

K = Crystalline-shape factor = 0.9

λ= X-ray wavelength, 1.5418 Å for Cu$K\alpha$

θ = Observed peak angle, degree

β = X-ray diffraction broadening, radian

The X-ray diffraction broading (β) is the pure width of the powder diffraction, free of all broadening due to the experimental equipment. α-alumina is used as a standard sample to observe the instrumental broadening since its crystallite size is larger than 1000 Å. The X-ray diffraction broadening (β) can be obtained by using Warren's formula.

From Warren's formula:

$$\beta = \sqrt{\beta_M^2 - \beta_S^2} \qquad \textit{(F.2)}$$

Where β_M = Measured peak width in radians at half peak height

β_S = Corresponding width of a standard material

Example: calculation of the crystallite site of TiO_2 calcined at 350°C

The half-weight width of (101) diffraction peak = 1.05°

= 0.0183 radian

The corresponding half-height width of peak of α-alumina = 0.004 radian

The pure width = $\sqrt{\beta_M^2 - \beta_S^2}$

= $\sqrt{0.0183^2 - 0.004^2}$

= 0.0178 radian

β = 0.0178 radian

2θ = 25.4°

θ = 12.25°

λ = 1.5418 Å

The crystallite size = $\frac{0.9 \times 1.5418}{0.0178 \cos 12.25}$

= 79.77 Å

= 7.977 nm

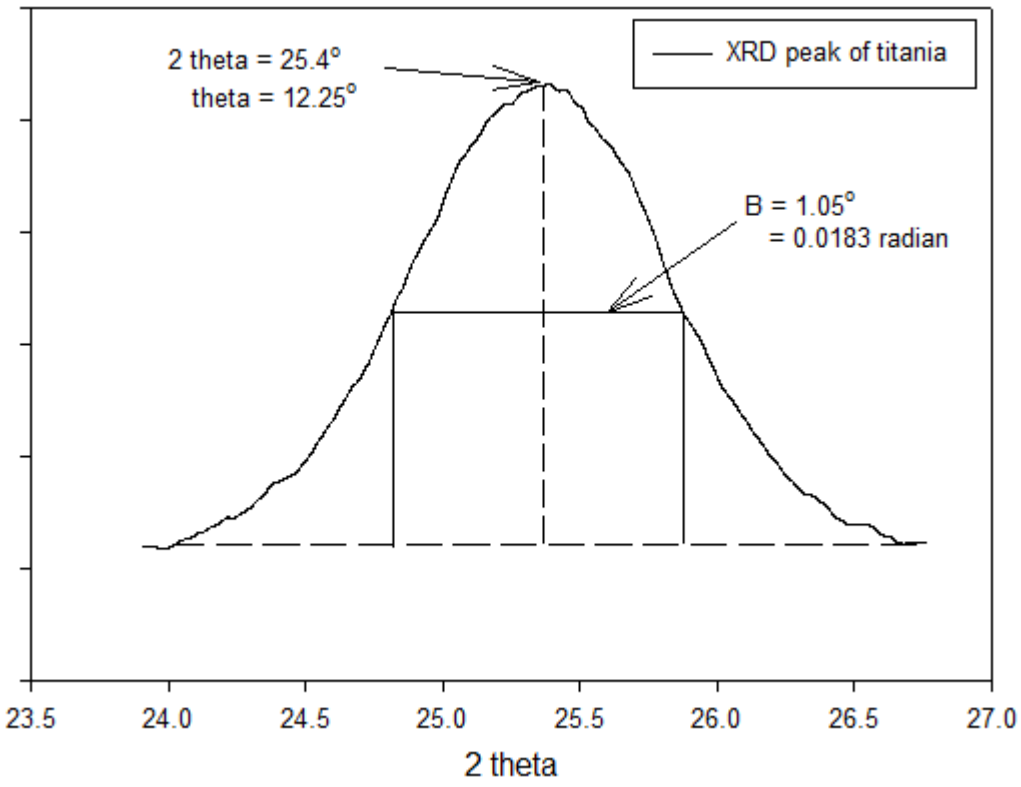

Figure F.1 The (101) diffraction peak of TiO_2 for calculation of the crystallite size

REFERENCES

APPENDIX

VITA

Mr.Warawut Waiwasa was born on august 6th, 1990 Ayutthaya, Thailand. He finished high school in from Ayutthaya Wittayalai School and received the bachelor's degree of Chemical Engineering from Faculty of Engineer, king mongkut's university of technology thonburi. He continued his master's study at Dapartment of Chemical Engineering, Faculty of Engineering, Chulalongkorn University.